ELSEVIER

Micron 36 (2005) 483–502

micron

www.elsevier.com/locate/micron

Review

Microscopy and single molecule detection in photosynthesis

Frantisek Vacha[a,b,*], Ladislav Bumba[b,1], David Kaftan[a,c], Martin Vacha[d]

[a]*Institute of Physical Biology, University of South Bohemia, Branisovska 31, 370 05 Ceske Budejovice, Czech Republic*
[b]*Institute of Plant Molecular Biology, Academy of Sciences of the Czech Republic, Branisovska 31, 370 05 Ceske Budejovice, Czech Republic*
[c]*Institute of Landscape Ecology, Academy of Sciences of the Czech Republic, Zamek136, 373 33 Nove Hrady, Czech Republic*
[d]*Department of Organic and Polymeric Materials, Tokyo Institute of Technology, Ookayama 2-12-1-S8, Meguro-ku, Tokyo 152-8552, Japan*

Received 28 February 2005; revised 18 April 2005; accepted 19 April 2005

Abstract

Progress in various fields of microscopy techniques brought up enormous possibilities to study the photosynthesis down to the level of individual pigment–protein complexes. The aim of this review is to present recent developments in the photosynthesis research obtained using such highly advanced techniques. Three areas of microscopy techniques covering optical microscopy, electron microscopy and scanning probe microscopy are reviewed. Whereas the electron microscopy and scanning probe microscopy are used in photosynthesis mainly for structural studies of photosynthetic pigment–protein complexes, the optical microscopy is used also for functional studies.

Keywords: Photosynthesis; Confocal microscopy; Single molecule spectroscopy; Electron microscopy; Scanning probe microscopy

Contents

* Corresponding author. Address: Institute of Physical Biology, University of South Bohemia, Branisovska 31, 370 05 Ceske Budejovice, Czech Republic. Tel.: +420 387 775 533; fax: +420 385 310 356.
E-mail address: vacha@jcu.cz (F. Vacha).
[1] Present address: EXBIO Praha, Nad Sahnou II 366, 252 42, Vestec u Prahy, Czech Republic

0968-4328/$ - see front matter © 2005 Elsevier Ltd. All rights reserved.
doi:10.1016/j.micron.2005.04.004

1. Introduction

Microscopy techniques were, from their very beginnings, one of the most frequently used techniques in plant research. In the past, the application was limited mainly to the light microscopy for plant anatomy research; however, with the progress in this field that has been achieved during the last century more beneficial studies have appeared. Development of fluorescence microscopy and confocal microscopy on the side of optical microscopy methods and electron microscopy, scanning probe microscopy and other advanced techniques on the side of the non-optical microscopy methods has boosted the research to higher and higher resolutions ending up at the level of single molecules.

Photosynthesis is a biological process in which the energy of light radiation is converted into the energy of chemical bonds. Primary processes of photosynthesis take place in pigment–protein complexes of thylakoid membranes of plant or algae chloroplasts, cyanobacteria and photosynthetic bacteria. Photosynthetic pigment–protein complexes can be divided according to their function into several groups: light-harvesting complexes that collect the light energy and transfer it to reaction centres, type I and type II photosystem complexes with their reaction centres as the sites of primary processes of energy conversion and various cytochromes that have mainly a transport role for the electrons released during the primary processes of charge separation in reaction centres. Distribution and arrangement of pigment–protein complexes (photosystems and light-harvesting complexes) in various types of photosynthetic organisms (bacteria, cyanobacteria, algae and higher plants) is shown in Fig. 1.

Photosynthetic pigment–protein complexes bear typically several chlorophyll like molecules (chlorophylls or bacteriochlorophylls) accompanied by various carotenoids. Usually, they are constituted as multiprotein complexes that can be further integrated in multiunit super-complexes and form larger membrane domains. In chloroplasts, thylakoid membrane is organised into two different grana and stroma regions. Stroma regions are characterised as free floating

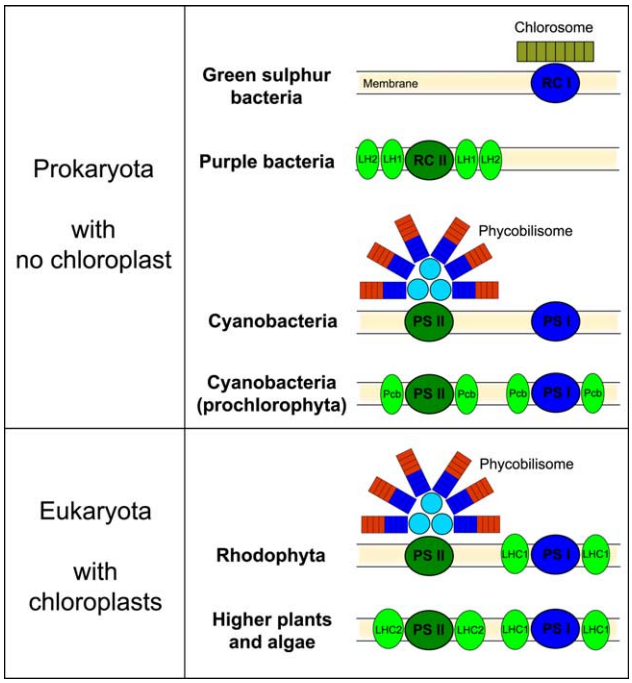

Fig. 1. Schematic representation of principal pigment–protein complexes of photosynthetic membranes from photosynthetic bacteria, cyanobacteria, algae and higher plants. Green sulphur bacteria contain reaction centres of type I with extra-membrane light-harvesting antennae complexes, chlorosomes. Purple bacteria contain reaction centres of type II with two major types of membrane light-harvesting complexes LH1 and LH2. Photosynthetic apparatus of cyanobacteria, red algae (Rhodophyta), green algae and higher plants consists of photosystem I (PS I), photosystem II (PS II) and various membrane or extra-membrane light-harvesting antennae complexes. In this figure, photosynthetic membrane is represented by black double line coloured in between in auburn. Blue ellipsoids represent photosystem of type I (PSI, photosystem I; RC I, reaction centre of type I), dark green ellipsoids represent photosystem of type II (PSII, photosystem II; RC II, reaction centre of type II), light green ellipsoids represent various types of membrane light-harvesting complexes. Phycobilisomes, the extra-membrane light-harvesting complexes are represented by blue and red rods anchored by light blue spheres, chlorosomes are represented by green-brown rod.

membranes, grana are formed by several membranes stacked together. The distribution of photosynthetic pigment–protein complexes in these two regions is different. Whereas cytochromes are distributed equally, grana regions are predominantly formed by photosystem II with its light-harvesting complexes and stroma regions contain mainly photosystem I complexes. Thanks to the presence of chlorophyll like pigments in photosynthetic pigment–protein complexes these complexes exhibits distinctive absorption and fluorescence properties in the visible and near infrared range of the electromagnetic spectrum. This feature can be utilised in favour of optical microscopy studies on the level of whole cell or chloroplasts or individual single pigment–protein complexes or molecules.

2. Optical microscopy

2.1. Wide field and confocal microscopy

Due to its limits in spatial resolution wide field microscopy was used in photosynthesis research only to study the plant anatomy or larger entities such as plant tissues, plant cells or the subcellular structures. However, with the invention of fluorescence microscopy and single molecule spectroscopy techniques the wide field microscopy retrieved its position in the field of super-resolution techniques as the one for single molecule detection (see in later chapter).

Confocal microscopy has brought up extended applications into the field cell biology. Its possibilities for obtaining high resolution images of very this sections of biological material and reconstructing them into 3-dimensional architectures of tissues, cells and organelles allow us to study both the cellular and subcellular structures or dynamic events. In spite of a great potential of confocal microscopy, only a few studies have appeared so far using this technique in photosynthesis research.

Relevant part of the applications of confocal microscopy in photosynthesis research is oriented in the single molecule detection and spectroscopy research and is discussed in later chapter. However, confocal microscopy has also been used in studies of larger photosynthetic units than single molecules of protein complexes. It was introduced mainly as a new methodology to re-evaluate the structure of chloroplasts in vivo. The fluorescence of chlorophyll molecules attached to pigment–protein complexes of photosynthetic apparatus may be used in the confocal microscopy to study chloroplasts and their ultra-structure. Along with the structural studies, the work on the origin of the chloroplast fluorescence as an emission of photosystem II pigment–protein complexes located in grana stacks of the thylakoid membrane was another main application of confocal microscopy in photosynthesis research (Van Spronsen et al., 1989; Sarafis, 1998; Hepler and Gunning, 1998; Mehta et al., 1999; Gunning and Schwartz, 1999; Osmond et al., 1999; Vacha et al., 2000).

Confocal microscopy has been also used to study diverse distribution of photosynthetic pigment–protein complexes in different cells of C4 plants of chloroplast thylakoid membranes (Pfundel and Neubohn, 1999). Near-field scanning fluorescence microscopy has been used to study fluorescence lifetimes of photosynthetic membranes of *Chlamydomonas reinhardtii* deficient in both Photosystem I and Photosystem II with picosecond resolution on nanometer scales (Dunn et al., 1994). Later, aperture-less scanning near-field microscope with femtosecond pulse exciation has been used to image photosynthetic membranes via two-photon absorption (Sanchez et al., 1999).

2.2. Principles in single molecule detection and spectroscopy

Current microscopic techniques allow fluorescence detection and fluorescence spectroscopy of single organic molecules, macromolecules, semiconductor nanocrystals and biological complexes. The methods are based on spatial isolation of individual objects in extremely diluted samples where neighbor-to-neighbor distances exceed the diffraction limit. Alternatively, samples may be cooled down to cryogenic temperatures and individual molecules can be isolated spectrally. In any case, high numerical aperture collection optics and sensitive detectors combined in wide-field fluorescence microscopy, scanning confocal microscopy or near-field scanning probe microscopies are the necessary tools for optical studies at single molecule levels. A recent review of this rapidly expanding field has been written by Kulzer and Orrit (2004).

Single molecule detection offers several ways to overcome the diffraction limit in determining and tracking the spatial position of individual objects. They are based on the fact that the centre of a diffraction-limited image (point-spread function) produced by a point-like emission source can be theoretically measured with unlimited accuracy. The practically achieved accuracy depends on the signal-to-noise ratio, number of pixels of the detector and overall stability of the apparatus. In one of the early studies, lateral accuracy of 30 nm with time resolution of 5 ms has been demonstrated (Schmidt et al., 1996). Very recently, the technique has been improved to distinguish steps in molecular motion as small as 1.5 nm, and used to study the mechanism of myosin (Yildiz et al., 2003) and kinesin (Yildiz et al., 2004) mobilities.

Apart from following the position of a single molecule, it has been also possible to co-localize several molecules within the same diffraction-limited spot by measuring the changes in the image pattern produced by discrete photobleaching of individual chromophores. Gordon et al., 2004, demonstrated reliable localization of two molecules separated by 10–20 nm long DNA strands, while Qu et al. (2004) managed to co-localize up to five molecules with

<10 nm resolution. These techniques are potentially important in the study of biological processes as they bridge the gap between distances measurable by resonant energy transfer (<10 nm) and the diffraction-limited resolution (>200 nm).

Co-localization based on photobleaching is somewhat limited by the necessity of observing the right sequence of photobleaching events, and by the complexity of the diffraction limited image with increasing number of molecules within the measured spot. These difficulties can be overcome at low temperatures by making use of the extremely sharp absorption lines of individual molecules at temperatures of liquid helium. Molecules localized in the same diffraction spot can be then separated spectrally, and each molecule is associated with an unperturbed image. In such measurements the number of molecules that can be localized within the diffraction spot is limited mainly by the ratio of inhomogeneous-to-homogeneous linewidths, and might theoretically reach hundreds to thousands. In the pioneering experiments, co-localization of seven molecules in three-dimensional space has been demonstrated (Van Oijen et al., 1998a, 1999a).

Conventional polarization microscopy measures projection of orientation angles into the object plane. With the progress of single molecule detection methodology, several techniques have been introduced that enable the determination of full 3-dimensional orientation of molecular transition dipole moments with accuracy of a few degrees. The orientation can be probed either via absorption or emission dipole moments. Apart from the special case of chromophores with high symmetry, such as semiconductor nanocrystals, where the orientation determination is straightforward (Empedocles et al., 1999), the methods for 3-dimensional orientation are based either on scanning or wide-field imaging microscopic techniques. The scanning techniques have in common the interaction of the molecular dipole moment with a characteristic and well-defined electric field profile in the focus of the microscope. The profile can be produced by annular illumination (Sick et al., 2000), by radial polarization of the excitation beam (Novotny et al., 2001) or by phase plate and amplitude mask modulation (Azoulay et al., 2001). A characteristic field profile which can be used for 3-dimensional orientation measurement is also present in the vicinity of a scanning tip in near-field scanning microscopy (Betzig and Chichester, 1993). An alternative approach towards the non-imaging techniques is the use of split excitation with four different polarizations combined with two orthogonally polarized detection paths. This technique has been recently used to study structural dynamics of single molecules of myosin V (Forkey et al., 2003).

One way to obtain the 3-dimensional orientations in the imaging methods is to fit defocused fluorescence images measured with a reflection objective lens at low temperatures (Sepiol et al., 1997), or by fitting aberrated fluorescence images in total internal reflection microscopy (Bartko and Dickson, 1999). Molecular dipole orientations can be also measured by fluorescence imaging using a combination of polarization modulated far and near-field excitation (Vacha and Kotani, 2003), by imaging emission patterns in the back focal plane of a high N.A. objective (Lieb et al., 2004) or by single molecule 'tomography' using five different directions of linearly polarized excitation light (Prummer et al., 2003). A theoretical account proposing the use of three detectors to measure fluorescence anisotropy and thus determining rapidly the dipole orientations has also been published (Fourkas, 2001).

2.3. Single molecule detection and spectroscopy in photosynthesis

Single molecule spectroscopy offers a unique possibility to study those photophysical processes and function related properties of photosynthetic systems that are otherwise hidden in the ensemble average. Below are reviewed the main results obtained in the past decade.

2.3.1. Bacterial light-harvesting complexes (LH2 and LH1)

By far the most studied photosynthetic units are light-harvesting complexes of purple photosynthetic bacteria. This is mainly because their structure has been known from crystallographic experiments for some time now, and it is thus possible to relate the well defined structural information with the expected spectroscopic and functional properties.

The light-harvesting 2 complex (LH2) of the purple bacterium *Rhodopseudomonas acidophila* consists of 27 bacteriochlorophyll a (BChl a) molecules that form two ring shaped sub-structures, B800 and B850, situated on top of each other. The B850 ring consists of 18 strongly interacting BChl a molecules arranged face-to-face and parallel to the symmetry axis of the complex. The nine BChl molecules in the B800 ring lie perpendicular to the symmetry axis. Light absorbed by the B800 ring is rapidly transferred (within 1 ps at room temperature) to the B850 ring. Photobleaching study of individual LH2 immobilized on charged surfaces at room temperature confirmed the strong interaction within the B850 ring (Bopp et al., 1997) as photobleaching of a single BChl a molecule within the ring led to complete quenching or the ring fluorescence. Polarization study on the same system revealed a breakdown of the ring circular symmetry on charged surfaces, with the resulting ellipticity fluctuating on the scale of seconds (Bopp et al., 1999).

A variety of spectroscopic information can be obtained by cooling the samples down to temperatures of liquid helium where homogeneous broadening of absorption and emission lines is strongly suppressed. The first experiments on B800 rings revealed sharp absorption lines attributable to single BChl a molecules within the ring, and heterogeneities between individual complexes (Van Oijen et al., 1998b). Further detailed studies on the B800 yielded the amount of disorder within the ring and time fluctuations of this

disorder. It was further shown that electronic energy is efficiently transferred between individual pigments within the ring (Van Oijen et al., 2000). In contrast to the B800 ring, the strong coupling between the BChl a molecules in the B850 ring leads to complete delocalization of the excitation over the whole ring (Fig. 2). This phenomenon is nicely manifested in the observation of several well-resolved broad spectral bands corresponding to different excitonic transitions (Van Oijen et al., 1999b). The spectra allow for distinction between random intra- and intermolecular disorder, and indicate that an additional systematic elliptic deformation must be taken into consideration to account for the observed spectral features (Ketelaars et al., 2001). Further insights into the dynamics of the disorder within the B850 ring has been obtained by measuring polarization of the fluorescence emission in a temperature range between 7 K and room temperature (Tietz et al., 1999, 2000).

The light-harvesting 2 complex of *Rhodospirillum molischianum* contains 24 BChl a molecules, eight of which are arranged in a planar B800 ring, similar in structure to that of *Rhodopseudomonas acidophila*. Orientations of the transition dipole moments of individual BChl

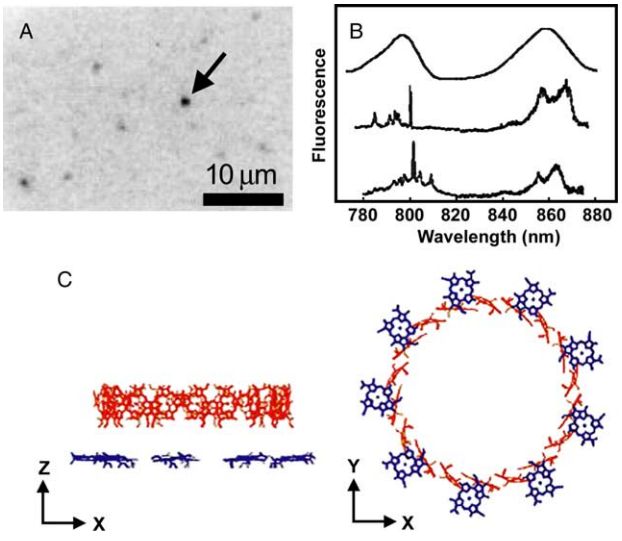

Fig. 2. (A) Wide-field fluorescence image of a $35\times25\ \mu m^2$ region of a polymer film doped with outer light harvesting complex (LH2) of *Rhodopseudomonas acidophila*. The illumination wavelength is 798 nm at an intensity of 125 W/cm^2. The fluorescence at $\lambda=890\pm10$ nm is detected with an intensified CCD camera after passing suitable filters. The black dots represent single LH2 complexes in resonance with the excitation (Van Oijen et al., 1998b). (B) Comparison of fluorescence-excitation spectra for an ensemble antennae complexes LH2 (top trace) and two individual LH2 complexes at the temperature of 1.2 K. The spectra are offset for clarity (Ketelaars et al., 2001). (C) Geometrical arrangement of the 27 bacteriochlorophyll molecules (BChl a) of the antennae complex LH2 of purple bacteria *R. acidophila* obtained by X-ray crystallography. The BChl a molecules form two rings with different function and properties. The BChl a molecules absorbing at 800 nm (B800) are depicted in blue, BChl a molecules absorbing at 850 nm (B850) are red. The phytol chains of the BChl a molecules are omitted for clarity (Ketelaars et al., 2001).

a measured within the B800 ring provided information on the strength of intermolecular intra-ring coupling and its spatial and temporal heterogeneities (Hofmann et al., 2003a). Detailed study of the temporal changes in the positions of absorption lines of individual molecules in the B800 ring reveal part of the energy landscape of the surrounding proteins. Three hierarchical energy levels and the corresponding characteristic fluctuation timescales have been observed (Hofmann et al., 2003b).

In contrast to LH-2 complex, the structure of the light-harvesting-1 (LH1) complex has only been studied with medium resolution. It is believed that various bacterial strains contain between 23 and 32 BChl a molecules arranged in a symmetric circular pattern. Low temperature excitation spectra of single LH-1 complexes of *Rhodopseudomonas acidophila* provided evidence for strong coupling between individual BChl a molecules, similar to that in the B850 ring of LH-2. Unlike LH-2, the spectra of LH-1 showed large variations in the number of spectral bands, their widths and polarization (Ketelaars et al., 2002). For the LH-1 complex of *Rhodospirillum rubrum* it has been shown that the distribution of conformational states in membrane-reconstituted complexes is much narrower than that for corresponding complexes solubilized in a detergent (Gerken et al., 2003a). Similarly, it has been found that interaction of the LH-1 complex with reaction center leads to stabilization of the circular symmetry of the structure (Gerken et al., 2003b).

Finally, the process of energy transfer from LH2 to LH1 has been studied in single photosynthetic units of the bacterium *Rhodobacter sphaeroides*, consisting of LH2, LH1 and reaction center. The results indicate that these constituents self-aggregate into stable formations in detergent suspension (Hofmann et al., 2003c).

2.3.2. Light-harvesting complexes of cyanobacteria

Phycobilisomes, the light-harvesting structures of cyanobacteria and red algae, contain several types of pigments–protein complexes, most often phycocyanins, allophycocyanins and phycoerythrins. In an early work, photobleaching of single B-phycoerythrin molecules containing 34 bilin chromophores in solution has revealed that photolysis of the complex occurs in a single step and that the B-phycoerythrin molecule behaves as a single quantum system rather than a collection of 34 independent chromophores (Wu et al., 1996). Energy transfer within single monomers of phycoerythrocyanin has also been studied and a dark state responsible for the observed blinking behavior has been identified (Zehetmayer et al., 2002, 2004). Polarized excitation of fluorescence of single allophycocyanin trimers, molecules with a three-fold symmetry, led to the observation of independent photobleaching of individual monomers. It has been suggested that two-photon mechanism involving exciton–exciton annihilation is responsible for the generation of exciton traps and for photobleaching (Ying and Xie, 1998).

2.3.3. Photosystem I and II pigment–protein complexes (PSI and PSII)

Single molecule studies on pigment–protein complexes of Photosystems I and II of higher plants and cyanobacteria have been rare so far, a fact that might be related to the lack of structural data and to the relative difficulty in detecting the main pigments in these systems, chlorophyll a (Chl a) and chlorophyll b (Chl b) on single molecule level. Energy transfer within the core antenna complex and from this complex to the reaction center of Photosystem I of *Synechococcus elongatus* has been studied on single entity level by temperature activated fluorescence quenching and low temperature spectroscopy (Jelezko et al., 2000). Study of monomeric and trimeric forms of light-harvesting complex II (LHCII) of higher plants revealed a distortion of the three-fold symmetry in the LHCII trimers and indicated weak interaction between the respective monomeric units (Tietz et al., 2001). Differences in the photobleaching and polarization characteristics have also been observed between native and mutated forms of the LHCII trimers (Gerken et al., 2002).

2.3.4. Light-harvesting chlorosomes of green bacteria

Supramolecular light-harvesting complexes (chlorosomes) of green sulfur bacteria are comprised of hundreds of molecules of bacteriochlorophyll c (BChl c) self-assembled into lamela-like structures (Psencik et al., 2004). Spectroscopy at room temperature of single chlorosomes of the bacterium *Chloroflexus aurantiacus* showed broad emission bands that change very little from chlorosome to chlorosome (Saga et al., 2002a). In contrast, emission spectra from individual chlorosomes of the bacterium *Chlorobium tepidum* vary considerably in peak position and widths. The differences have been ascribed to slightly different forms of the BChl c pigments present in both bacteria (Saga et al., 2002b).

3. Electron microscopy

Electron microscopy (EM) is widely used technique for studying the biological structures at resolutions spanning from molecular to near atomic. When applied to proteins, EM cannot compete with X-ray or NMR techniques in terms of resolution but it is very useful for studying the structure and function of individual macromolecules, their oligomers and supramolecular assemblies. EM is also of great value in time-resolved studies, in analysis of different functional states, and in studying conformational flexibility in large complexes.

Imaging of biological objects in an electron microscope is similar in many ways to the imaging in a light microscope. The key differences in a technology of electron microscopic imaging are that the interacting radiation is composed by electrons instead of photons, and that the lenses are magnetic instead of optical. The resolution of the transmission electron microscope is about 1 Å, much lower than the value of 0.04 Å that imply from the wavelength of electrons. It is restricted by a small aperture size needed because of aberrations in the electromagnetic lenses. Small apertures give a large depth of field that produces images of a two-dimensional (2D) projection from a 3D structure of the observed specimen. The structure can be then recovered from a set of projections from different view directions by tomographic reconstruction (Saibil, 2000).

The main difficulties in imaging macromolecules are radiation sensitivity, specimen movement in the electron beam and low contrast. These effects have so far limited the resolution of macromolecular imaging to about 3 Å in the best cases. Since electron micrographs of biological molecules are very noisy, substantial improvement of image quality can be obtained by averaging of individual projections (Subramaniam and Milne, 2004). Averaging procedures can be divided into crystallographic and non-crystallographic methods and both were employed in structural studies of photosynthetic membrane protein complexes. Crystallographic methods are based on analysis of 2D crystals of rather small proteins and have the potential to solve structures to the atomic resolution. Non-crystallographic methods use averaging of single particle projections with a resolution limit that is restricted to about 10–25 Å (single particle analysis).

The specimen preparation method is one of the factors that strongly determine the resolution. Purified photosynthetic complexes are very volatile and, in addition, extensive detergent treatment or time exposure usually cause the dissociation of a part of the complex, for example in protein complexes known as peripheral light-harvesting antennae. Furthermore, some of the proteins themselves are intrinsically unstable, for example the D1 protein of Photosystem II complex has a half-life of approximately 30 min in moderate light (Barber and Andersson, 1992).

The proteins are composed of light atoms (C, H, O, N, etc.) that scatter electrons weakly, producing images with low contrast. Negative staining with heavy atom salts, such as uranyl acetate, is a simple technique to improve the contrast (Boekema, 1991; Harris and Scheffler, 2002). Sample is placed on carbon coated EM grid that may have been glow-discharged to improve the hydrophilicity of the carbon film and, therefore, increase the quality of specimen adhesion to the grid. Negative stain surrounds the molecules and space cavities within the protein but it does not penetrate the protein interior. As a result, the negative staining shows with a good contrast only the protein surface with a maximal resolution limited to about 15 Å.

Cryo-electron microscopy (cryo-EM) is a high-resolution imaging technique that is particularly appropriate for the structural determination at atomic resolution (Henderson, 2004). In cryo-EM, sample is embedded in a thin layer of vitreous ice formed by rapid freezing of the sample in liquid ethane. The major advantages of cryo-EM

lie in imaging of macromolecules in their native state as well as protecting them from damage by the electron beam. Moreover, the contrast directly originates from protein density rather than from surrounding stain and it allows structure determination to a sufficient resolution up to 3.5 Å. To enhance the contrast of the sample in cryo-EM a cryo-negative stain sample preparation method has been recently introduced (Adrian et al., 1998).

3.1. Electron crystallography

Unlike X-ray crystallography, which typically requires large 3D crystals, electron microscopy is ideally suited to study 2D crystalline objects. This makes electron crystallography particularly powerful technique when applied to structural studies of membrane proteins (Walz and Grigorieff, 1998). One of the limits of the structure determination at high resolution is the production of the well-ordered and large 2D crystals. Unlike the bacteriorhodopsin that forms regular 2D arrays in vivo within the native membranes (Unwin and Henderson, 1975) 2D crystals of most of membrane proteins must be introduced artificially by incubating proteins with a lipid detergent mixture and subsequent removal of detergent either by dialysis or hydrophobic adsorption (Kühlbrandt, 1992; Rigaud et al., 2000; Mosser, 2001). Recorded images and electron diffraction patterns are computationally processed and the resulting data merged into a final 3D map of the protein.

The essential principles of electron crystallography techniques came from the analyses of 2D crystals of bacteriorhodopsin, a light-driven proton pump from cytoplasmatic membrane of extreme halophyte purple bacterium *Halobacterium salinarium*. The atomic structure of bacteriorhodopsin was first determined by electron crystallography to 3.5 Å (Henderson et al., 1990) and subsequently refined to 3 Å resolution (Grigorieff et al., 1996).

The plant light-harvesting complex is another example of an atomic model that has been built entirely on the basis of electron crystallographic analysis at 3.4 Å resolution (Kühlbrandt et al., 1994). The model gave a more detailed structural picture of LHCII and became one of the most important features in photosynthetic research in the last ten years. Recently, the structure of spinach LHCII at higher resolution was determined by using X-ray crystallography at 2.72 Å resolution (Liu et al., 2004).

3.1.1. Photosystem I (PSI)

The 2D crystals of spinach PSI were produced by partial detergent treatment of thylakoid membranes giving the projection map of the higher plant PSI complex at about 25 Å resolution (Kitmitto et al., 1998). The projection structure showed the overall shape of the complex with high density domain ('ridge') on the stromal side that was assigned to contain the extrinsic polypeptides. The recent studies on 2D crystals of higher plant PSI have also revealed the binding sites of mobile electron carriers such as ferredoxin (Ruffle et al., 2000) and plastocyanin (Ruffle et al., 2002). Recently, X-ray structure at 4.4 Å for higher plant PSI complex from pea (*Pisum sativum*) has been reported (Ben-Shem et al., 2003).

In contrast to the higher plants, more structural studies were done on the more robust cyanobacterial PSI complex. Both 2D and 3D crystals of the cyanobacterial PSI complex have been reported in the last 15 years. The first 2D crystals of cyanobacterial PS I were investigated by Ford et al., 1990. This and further work on 2D crystals of PS I from cyanobacteria unraveled the common molecular shape of the trimeric cyanobacterial PS I complex (Böttcher et al., 1992). Later studies on 2D crystals of monomeric PSI have yielded a 3D map to 8 Å resolution (Karrasch et al., 1996). However, much earlier the 3D structure of PSI was determined to the resolution of 6 Å by X-ray crystallography (Krauss et al., 1993) and recently the structure of cyanobacterial PSI complex was resolved to 2.5 Å resolution with the same technique (Jordan et al., 2001).

3.1.2. Photosystem II (PSII)

Many reports concerning 2D crystallography of PSII have been published and recently reviewed by Bumba and Vácha (2003). Generally, three approaches were employed for structural analysis of PSII 2D crystals: (i) analysis of the PSII crystalline arrays in the native thylakoid membrane, (ii) in situ crystallization procedures including detergent-induced delipidation of PSII-enriched membranes, and (iii) reconstitution of isolated PSII complexes with thylakoid lipids.

Electron micrographs of isolated granal membrane regions enriched in PSII complexes showed that PSII particles can be organized in 2D arrays (e.g. Staehelin, 1976; Stoylova et al., 2000; Ford et al., 2002). Analysis of the 2D crystalline areas have provided structural details about the organization of PSII and LHCII complexes in grana membranes. The lattice parameters slightly varied among the reports, but single unit cell showed significant similarities. The unit cell contained dimeric PSII with relatively large stain density areas that were attributed to include the light-harvesting proteins (Fig. 3). These data suggested that the basic unit contains dimeric PSII associated with two or three additional trimeric LHCII in spinach (Boekema et al., 2000a) or four LHC trimers in *Arabidopsis thaliana* (Yakushevska et al., 2001).

2D crystals of PSII were also induced by a detergent treatment of thylakoid membranes. Detergents preferentially solubilise non-stacked stromal regions of the membrane leaving grana membranes intact. The formation of the 2D crystals involves dissociation of LHCII from PSII to separate areas, specific associations between the PSII complexes, and gradual depletion of lipid molecules. Many different types of PSII 2D crystals have been obtained using a variety of detergents and analysed by both negatively stained preparations (Bassi et al., 1989; Santini et al., 1994; Ford et al., 1995; Marr et al., 1996; Lyon, 1998)

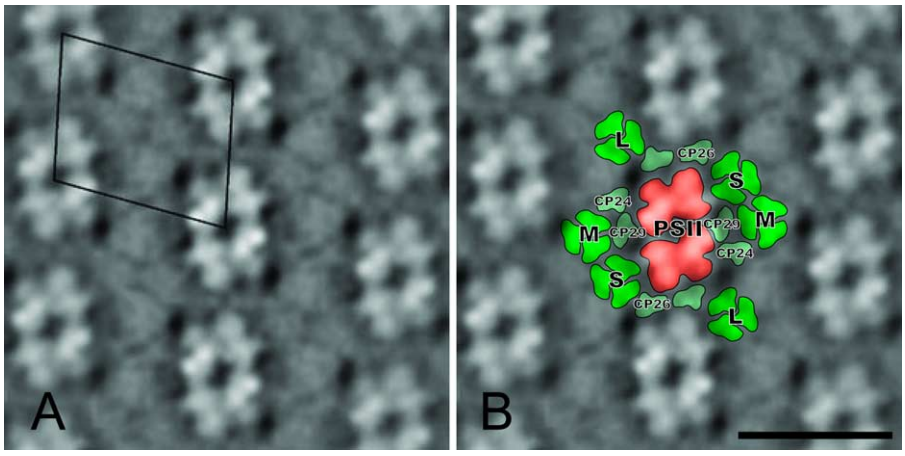

Fig. 3. Image analysis of the ordered supermolecular organization of Photosystem II complex with associated light-harvesting antenna (LHCII) in isolated thylakoid membrane fragments of *Arabidopsis thaliana*. (A) The sum of 450 images from plants with indicated unit cell or repeating motif (Yakushevska et al., 2001). (B) Contour version of the image with proposed position of various types of major trimeric LHCII complexes (S, M, L), and minor chlorophyll protein (CP) antennae CP29, CP26, and CP24 subunits. The scale bar is 20 nm.

or imaged under cryo conditions (Stoylova et al., 1997; Ford et al., 2002). Unfortunately, low resolution only shows that the unit cells contain dimeric PSII complex.

High resolution structural data of PSII have been obtained through the analyses of 2D crystals of purified PSII complexes. 2D crystals of spinach PSII subcomplex have been prepared by several groups (Dekker et al., 1990; Mayanagi et al., 1998). The crystals were analysed after negative staining and 3D models were constructed at a resolution of about 20 Å. Further improvement in crystal formation and the use of cryo-EM resulted in a 3D projection map of this subcomplex at 8 Å resolution (Rhee et al., 1998). This work revealed for the first time the organization of the transmembrane helices of the PSII complex protein subunits. Recently, a 3D structure of PSII core dimer from spinach has been reported at a resolution of about 10 Å (Hankamer et al., 2001). This 3D model has provided an overall picture of subunit organization in the PSII core complex consistent with an X-ray crystallography structure of cyanobacterial PSII complex (Zouni et al., 2001; Kamiya and Shen, 2003; Ferreira et al., 2004).

3.2. Single particle analysis

Single particle analysis offers a powerful means of visualizing the structure and dynamics of large proteins and macromolecular complexes, which are difficult to organize into 2D or 3D crystals. The sample is imaged as individual (single) particle at different orientations in the plane of the support film. To separate these various projections, particles are iteratively aligned, treated with multivariate statistical analysis and classified using a combination of algorithms before increasing their signal-to-noise ratio by averaging (Van Heel et al., 2000; Frank, 2002). A variety of methods use different views on the protein to yield all the information necessary to reconstruct the molecule (Ruprecht and Nield, 2001). The advantage of this technique is that it is not necessary to obtain a highly regular arrangement of the objects. Moreover, the structures of an extremely broad size range are suitable for investigation. The lowest theoretical size limit is at present ~100 kDa, determined by the requirement for accurate aligning of individual particles.

The method has been successfully used to carry out 3D reconstruction of many large macromolecular assemblies (e.g. viruses, ribosomes, chaperones) as well as membrane protein complexes (e.g. mitochondrial complex I by Grigorieff, 1998). However, the single particle approach has yielded structures to only medium resolution of about 10 Å. To bridge the resolution gap between X-ray crystallography and electron microscopy, a combination of single particle reconstruction with molecular docking of known X-ray coordinates of the component structures is a powerful way to approach the atomic structure of a large macromolecular complex (Roseman, 2000). Precise localization of individual subunit within the multisubunit complex can also be achieved by labeling with gold clusters (Büchel et al., 2001) or difference mapping (Heymann et al., 2003).

3.2.1. Photosystem I (PSI)

The structural investigations of PS I with electron microscopy started in the late 1970 s, when Newman and Sherman (1978) described the first rod-like particles assigned to PS I in the cyanobacterium *Synechococcus cedrorum*. Towards the end of the 1980 s, significant progress has been made in the structural studies of PSI (Fig. 4). In cyanobacteria, such as the thermophilic *Thermosynechococcus elongatus* and mesophilic *Synechocystis* PCC 6803, single particle analysis revealed that PS I can occur in two different oligomeric states, a monomeric and a trimeric form (Boekema et al., 1987; Ford and Holzenburg, 1988; Rögner et al., 1990). These forms are at least partly interchangeable and their existence depends on

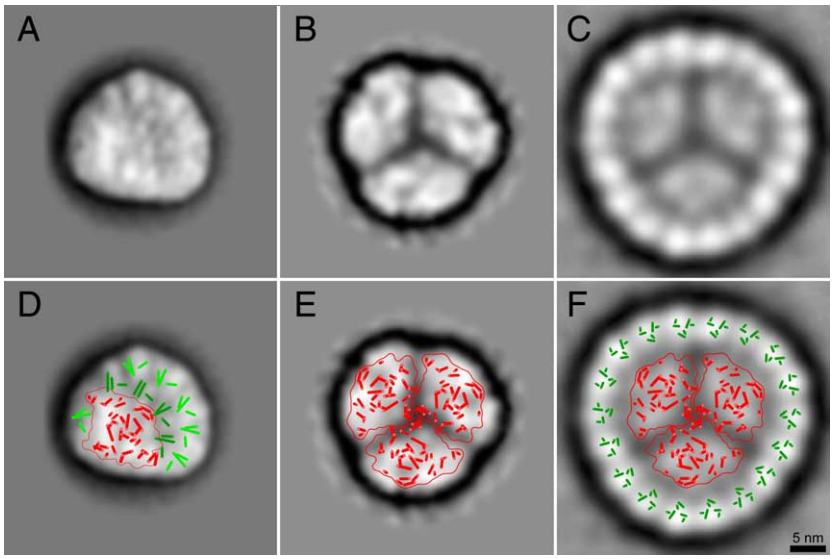

Fig. 4. Comparison of top view projection map of a supercomplex of Photosystem I associated with its light harvesting antennae complexes (PSI–LHCI) from (A and D) green alga *C. reinhardtii* (Germano et al., 2002); (B and E) trimeric PSI core complex from cyanobacterium *Synechocystis* PCC 6803 (Kruip et al., 1993); and (C and F) Pcb–PSI supercomplex from *Prochlorothrix hollandica* (Bumba et al., 2005). (D–F) The projections of A–C are overlaid with a patterns of Photosystem I core complex (red) and its light harvesting antenna proteins (green) to indicate their positions. (D) Top view projection map of the *C. reinhardtii* PSI–LHCI supercomplex overlaid with a X-ray model of the PSI-LHCI complex from pea bordered with a yellow contour (Ben-Shem et al., 2003) indicating monomeric PSI core complex (red) with the four tentatively assigned LHCI subunits (dark green). The PSI complex from *C. reinhardtii* has, when compared with the PSI from higher plants, additional 6 light-harvesting LHCI subunits (pale green) that have been modelled into the figure after inspection of the density profile and shape of the projected structure (Germano et al., 2002). (E) Top view projection map of the trimeric PSI complex from *Synechocystis* PCC 6803 with superimposed high-resolution X-ray model of the PSI complex from *Synechococcus elongatus* (Jordan et al., 2001). (F) Top view projection map of the *P. hollandica* Pcb–PSI supercomplex overlaid with a high-resolution X-ray model of the cyanobacterial trimeric PSI complex (Jordan et al., 2001) in the center of the complex (red) surrounded by 18 densities of the PcbC subunits modelled as transmembrane helices of the CP43 protein (green) of cyanobacterial photosystem II complex (Ferreira et al., 2004). Scale bar indicates 5 nm.

the environmental growth conditions. The trimeric organization of PS I has been shown for *Prochlorothrix hollandica*, an unusual cyanobacterium that contains also chlorophyll *b* molecules (Van der Staay et al., 1993). The side-view projection showed overall height of the complex with a ridge on the stromal side that was attributed to the extrinsic proteins. The precise location of these subunits was conducted by difference mapping of PSI with bound and without the extrinsic proteins (Kruip et al., 1993). Prior to the high resolution X-ray structure of PSI (Jordan et al., 2001), single particle analysis on deletion mutants was also helpful for the assignment of individual proteins in the PS I complex (Kruip et al., 1997).

In cyanobacteria, water soluble phycobilisomes act as peripheral antenna systems for both PSII and PSI under normal growth conditions. Under conditions of iron deficiency, a newly synthetized membrane-intrinsic chlorophyll *a*-binding protein encoded by the *isi*A gene replaces phycobilisomes in the peripheral antenna function. Recent electron microscopy studies revealed that 18 subunits of the IsiA protein form an antenna ring around the trimeric PSI core complex of *Synechocystis* PCC 6803 (Bibby et al., 2001a) and *Synechococcus* PCC 7942 (Boekema et al., 2001b). Similar proteins, known as Pcb, which bind both chlorophyll *a* and *b* molecules have also been found to form an 18-subunit light-harvesting antenna ring around trimeric PSI of the prochlorophyte *Prochlorococcus marinus* SS120 (Bibby et al., 2001b) and *Prochlorothrix hollandica* (Bumba et al., 2005).

PSI complex of higher plants and algae is associated with a peripheral antenna complex known as light-harvesting complex I (LHCI), belonging to the group of chlorophyll *a/b*-binding proteins of the Lhc super-family (Green and Durnford, 1996). In contrast to cyanobacteria, single particle analysis of isolated PSI from higher plants showed only monomeric particles without an apparent symmetry (Boekema et al., 1990). A comparison of the projection maps of higher plant PSI complex with cyanobacterial monomeric particle revealed that LHCI antennae proteins form a half-moon shaped antenna on one side of the PSI complex, the same side at which the peripheral IsiA and Pcb antenna proteins bind in cyanobacteria and prochlorophytes (Boekema et al., 2001a). Recent studies of the PSI–LHCI supercomplex have showed the size and arrangement of the LHCI antenna system in the green alga *Chlamydomonas reinhardtii* (Germano et al., 2002; Kargul et al., 2003).

3.2.2. Photosystem II (PSII)

Since there was a lack of high resolution structural data of photosystem II for such a long time, the single particle analysis has played a crucial role in structural studies of this

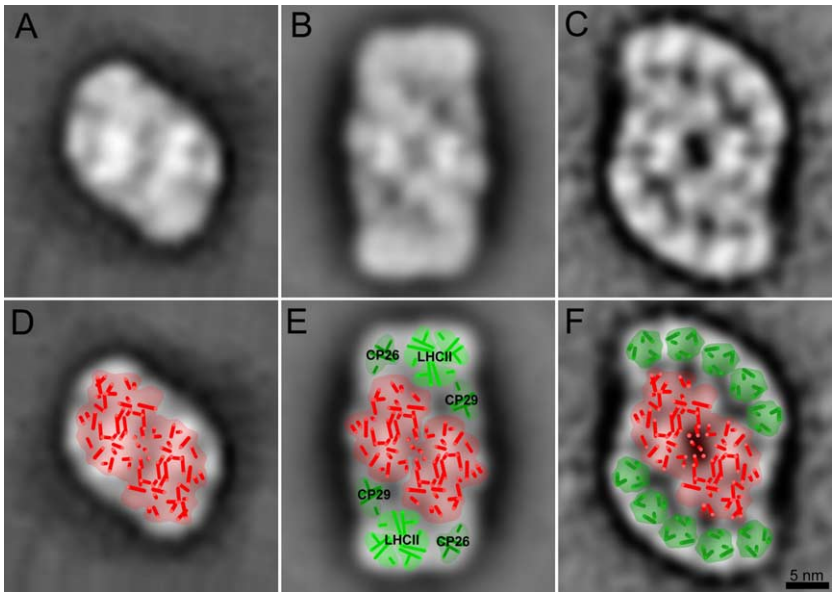

Fig. 5. Comparison of top view projection map of dimeric Photosystem II (PSII) complexes. (A and D) PSII complex from red alga *Porphyridium cruentum* (Bumba et al., 2004a). (B and E) Supercomplex of Photosystem II with associated major and minor antennae light harvesting proteins (PSII-LHCII) from spinach (Nield et al., 2000). (C and F) Pcb–PSII supercomplex from prochlorophyte *Prochloron didemni* (Bibby et al., 2003). (D–F) The projections of A–C are overlaid with a patterns of Photosystem II core complex (red) and its light harvesting antenna proteins (green) to indicate their positions. (D) Top view projection map of the dimeric PSII complex from red alga *Porphyridium cruentum* overlaid with a high-resolution X-ray model of the PSII complex (red) from cyanobacterium *Synechococcus elongatus* (Ferreira et al., 2004). (E) Top view projection map of the PSII–LHCII supercomplex from higher plants overlaid with a high-resolution X-ray model of the dimeric PSII complex (red) in the central region of the supercomplex. The flanking region on each side of the PSII dimer is attributed to chlorophyll *a*/*b*-binding antenna proteins modelled as one trimeric light harvesting complex (LHCII) (bright green) derived from X-ray data of Liu et al. (2004) and two monomeric chlorophyll protein (CP) antennae, CP29 and CP26 (dark green), that have been proposed as linker proteins between LHCII trimers and the PSII core complex. (F) Top view projection map of the *P. didemni* Pcb–PSII supercomplex incorporating the X-ray structures of the cyanobacterial PSII core dimer (red) (Ferreira et al., 2004). The flanking region accommodates five Pcb proteins along each edge of the dimer (green), making a total of 10 Pcb subunits per PSII dimer.

complex (Fig. 5). Single particle analysis of PSII has been dominated by studies of negatively stained specimens and the results were extensively reviewed in Hankamer et al. (1997) and recently by Bumba and Vácha (2003). The first studies concerning PSII structure have been published at the end of 1980s but a low number of averaged particles did not allow to recognize structural details (Dekker et al., 1988). Later, comparative projection maps of PSII core complex from both thermophilic cyanobacterium (*Thermosynechococcus elongatus*) and spinach were published (Boekema et al., 1995). The top-view class averages showed two-fold symmetry indicating a dimeric organization of the PSII core complex. The side-view projections showed small protrusions on the lumenal side of the complex that were attributed to the extrinsic proteins of the oxygen-evolving complex (Kuhl et al., 1999; Bumba et al., 2004a) and analysis of two core complexes interacting via their tips hints the possible arrangement of these core complexes in vivo (Kuhl et al., 1999).

The details of the organization of trimeric and monomeric light-harvesting complex (LHCII) around the PSII core complex were provided by the characterization of a PSII–LHCII supercomplex (Boekema et al., 1995). Single particle analysis indicated the dimeric PSII core complex surrounded by two peripheral antenna structures in symmetry-related positions, each consisting of one trimeric and two monomeric LHCII complexes. Biochemical analysis identified the monomeric LHCII proteins as CP29 and CP26 and the trimeric LHCII as a complex of the Lhcb1 and Lhcb2 gene products. Further studies on the PSII–LHCII supercomplexes have also increased our knowledge on the positions of the extrinsic proteins within the supercomplex (Boekema et al., 1998a) and conformational changes in the supercomplex upon removal of extrinsic subunits (Boekema et al., 2000b). Recently, the interaction of the PSII–LHCII supercomplexes has been studied in adjacent layers of stacked chloroplast thylakoid membranes (Bumba et al., 2004b). The use of single particle analysis with cryo-EM in the PSII field came to a 3D structure of the higher plant PSII–LHCII supercomplex at a resolution of 24 Å (Nield et al., 2000). This structure revealed the oxygen-evolving complex to have a tetrameric appearance, almost similar to that indicated in earlier freeze-etch studies at lower resolution (Seibert et al., 1987).

The associations of additional LHCII trimers to the PSII–LHCII supercomplex have been studied by a mild detergent treatment of the PSII-enriched membranes and single particle analysis (Boekema et al., 1998b; Yakushevska et al., 2001). These studies have shown trimeric LHCII to be attached in three different positions, referred to strongly (S),

moderately (M) and loosely (L) bound LHCII trimers (Boekema et al., 1999a). Two S-type trimers have been previously proposed to flank the dimeric PSII complex and altogether form the PSII–LHCII supercomplex. The latter two types (M and L) were associated on both sides of the supercomplex (Boekema et al., 1999b). Recently, location of the minor antenna proteins, CP26 and CP29, has been determined using comparison of the wild-type plants with those of lacking these subunits (Yakushevska et al., 2003).

4. Scanning probe microscopy

The concept of the scanned probe microscope (SPM) relies on a sharp stylus interacting through the atomic asperities with a sample; the XYZ piezoelectric transducer translates the probe over the imaged surface (or vice versa) at the angstrom to nanometre distance with the sub-nanometre accuracy. The tip–surface interactions are monitored during the raster scan allowing for the reconstruction of the surface topography and/or functional maps at or near the atomic level. Numerous SPMs based on this principle have been constructed, including the scanning tunnelling microscope (STM) (Binnig et al., 1982), atomic force microscope (AFM) (Binnig et al., 1986) or the scanning force microscope (SFM), scanning near field optical microscope (SNOM) (Pohl et al., 1988), scanning Kelvin probe microscope (SKPM) (Nonnenmacher et al., 1991) or scanning surface-potential microscope (SSPM), lateral force microscope (LFM), electric force microscope (EFM), magnetic force microscope (MFM) and others. This section reviews the major advancements in those branches of SPM that provided, within the time span of the recent decade, high resolution images of the structure and/or function of the photosynthetic membranes and the isolated light-harvesting antennae, photosystem complexes and reaction centres.

4.1. Scanning force microscopy

The SFM measures the forces acting between the sample's surface and the probe mounted on a flexible cantilever. The differential bending of the cantilever is monitored via optical system granting a force detection limit of ca. 10 pN or else vertical topographic resolution of 0.1 nm; lateral resolution of 1 nm has been frequently attained on reconstituted membrane proteins or even native membranes. The principles of the SFM techniques have been recently discussed within the context of their substantial impact on the advancements in biological sciences by Myhra (2004), Moreno-Herrero et al. (2004) and Braga and Ricci (2003), the dynamic atomic force microscopy has been reviewed in detail by Garcia and Perez (2002).

By its virtue, the microscope is capable to probe the nature and magnitude of the interactions involved in the recognition of the single ligand–receptor pairs (reviewed in Zlatanova et al., 2000) as well as probing the intramolecular interactions (Best et al., 2003). It is the microscope capacity to operate under aqueous solutions and the exceptional *S/N* ratio that has made the SFM the prime high resolution imaging tool of native membrane proteins (Mueller et al., 2002). The technique has further gained a major potential by successfully combining its imaging modes providing the surface topography with the measurements of local micro elasticity (Shao et al., 1997), light induced volume changes (Rousso et al., 1997), electron conductivity (Stamouli et al., 2004), electrostatic potential (Lee et al., 2000), phosphorylation levels (Liou et al., 2002) and by being paralleled by SNOM (Dunn et al., 1994; Trudel et al., 2001) and laser-scanning confocal microscopy (Gradinaru et al., 2004). The SFM probe has been used also as a nano-tool, capable of nanomanipulation of biological molecules and structures (reviewed in Fotiadis et al., 2002). This approach has been applied in disassembly of PSI super complexes (Fotiadis et al., 1998), bacterial reaction centre (Scheuring et al., 2003a) and probe the micro elastic properties of PSII (Shao et al., 1997).

Bacterial reaction centres with light-harvesting complexes (RC-LH1)

The reaction centre (RC) complex in photosynthetic purple bacteria is made up by the L and M transmembrane subunits, the extramembrane H subunit at the cytoplasmic and a tetraheme cytochrome complex (4Hcyt) at the periplasmic face of the RC. The RC is surrounded by the LH1 ring of 16 αβ transmembrane apoproteins (Roszak et al., 2003; Cogdell et al., 2004). The RC–LH1 complexes have been imaged at high resolution by the contact mode SFM in liquid only recently. Scheuring et al. (2003a) reports the lateral dimension of 104×98 Å for the elliptical RC–LH1 complex from *Rhodopseudomonas viridis* and later also the 100×90 Å RC–LH1 complexes of *Rhodospirillum photometricum* (Scheuring et al., 2004a). Fotiadis et al. (2004) have resolved the details of the intact RC–LH1 complex of *Rhodospirillum rubrum,* showing the RC complex of a total height of 94 Å. The position of the RC within the LH1 complex is clearly non-central in all the complexes imaged both from the periplasmic face in the RC–LH1 complexes of *Rhodopseudomonas viridis* (Scheuring et al., 2003a) and the *Rhodospirillum rubrum* (Fotiadis et al., 2004), as well as the cytoplasmic face in the RC-LH1-PufX dimers from *Rhodobacter sphaeroides* (Siebert et al., 2004) and the RC–LH1 complexes of *Rhodospirillum photometricum* (Scheuring et al., 2004a). The topography of the periplasmic side of the RC–LH1 complex imaged at a high applied force (200–300 pN) unveil the strongly asymmetrical×shaped structure of the L and M subunit surface (Fotiadis et al., 2004). Upon the nanodissection of the 4Hcyt subunit, the RC protrudes only 14.8±1.3 Å above the membrane in *Rhodopseudomonas viridis* (Scheuring et al., 2003a), while the RC–LH1 complexes devoid of the H subunit are completely enclosed

by the LH1 ring in *Rhodospirillum rubrum* (Fotiadis et al., 2004). The imaging of the extramembranal subunits represents always a challenge as the H subunits were readily removed from the complexes during the scan (Siebert et al., 2004). Nevertheless, Fotiadis et al. (2004) resolved the details of the cytoplasmic face of the intact RC–LH1 complex of *Rhodospirillum rubrum,* showing the H subunit bound asymmetrically to the intact RC complex protruding 40±3 Å above the membrane and reporting the LH1 rim to the RC top height difference of 22±2 Å. The RC–LH1 complex with the H subunit protrudes by 28±3 Å in *Rhodospirillum photometricum* (Scheuring et al., 2004a). Scheuring et al. (2003a) reports 50 Å width and 33 Å height of the 4Hcyt–RC–LH1 complex from *Rhodopseudomonas viridis*.

4.1.1. Inner bacterial light-harvesting complexes (LH1)

The hexadecameric ring of the 100 Å LH1 complex has been imaged in contact mode SFM, either as a part of the intact complexes of RC–LH1 or as the individual LH1 complexes devoid of RC. The periplasmic face of the empty elliptical LH1 of *Rhodopseudomonas viridis* has a central depression of 12.3±2.1 Å. The complex protrudes 6.7±1.3 Å above the membrane, contrasting with the 10.1±1.4 Å protrusion with the RC present. The αβ heterodimers exhibit a left hand twist with a lower peripheral part (Scheuring et al., 2003a). In the *Rhodospirillum rubrum*, LH1 complexes with discernible α and β subunits protrude 12±2 Å above the periplasmic membrane side and 19±2 Å above the cytoplasmic side (Fotiadis et al., 2004). The tapping mode SFM in liquid used by Bahatyrova et al. (2004) provided high resolution topography of the LH1 2D crystals of *Rhodobacter sphaeroides*, lacking long range crystalline arrays. About 86% of the LH1 complexes protruded with their periplasmic side up by 8±1 Å above the lipid, the cytoplasmic orientation protruded by 14±1 Å, having a smaller inner diameter. Three major size groups (116±5.6, 126±5 and 145±8 Å in diameter) corresponded to the 15, 16 and 18 putative αβ subunits. The notable heterogeneity in shapes and sizes of the complexes (41% elliptical, *b*/*a* ranging from 0.75 to 0.8 in medium to large rings, 35% circular, 19% polygonal, 5% open rings) points to the apparent complex flexibility, that is discussed in the light of the network of hydrogen bonds stabilising the $\alpha_1\beta_1$Bchl$_2$ units, including the implications for the shuttling of the quinone in and out of its Qb site through the LHI complex. Siebert et al. (2004) reports at least two populations of LH1 complexes in *Rhodobacter sphaeroides*: 113 Å wide intact RC–LH1 complexes and 134 Å rings of LH1 depleted of RC that may contain up to 18 $\alpha_1\beta_1$Bchl$_2$ subunits. Scheuring et al. (2004b) provided evidence that the PufX protein drives the dimerisation of the RC–LH1 complexes of *Rhodobacter sphaeroides* both in 2D crystals as well as in the non-crystalline areas of the membranes.

4.1.2. Outer bacterial light-harvesting complexes (LH2)

Contact mode SFM in liquid applying relatively large forces (up to 200 pN) was employed in imaging of the non-americ structure of the LH2 complex. In *Rubrivivax gelatinosus*, the 54 Å ring (*b*/*a*=0.95) protrudes 5.6±0.8 Å on the cytoplasmic face. The periplasmic face of the 49 Å ring (*b*/*a*=0.91) was identified by the decrease of protrusion from 13.9±1.7 to 8.9±1.4 Å (volume decreased from 3300 to 1800 Å^3) in the thermolysin digested C terminal extrinsic helical segment of the α-subunit on the membrane surface (Scheuring et al., 2001). Interestingly, Scheuring et al. (2003b) shows the 53 Å rings of LH2 complexes from *Rhodobacter sphaeroides* with nine subunits protruding 13.1 Å on the periplasmic face while at the cytoplasmic side, only four, 3.8 Å protruding subunits are discernable. Stamouli et al. (2003) imaged the 2D crystals of the 55±2 Å rings of LH2 complexes from *Rhodopseudomonas acidophila*, protruding 2.1±0.6 Å. Bahatyrova et al. (2004) confirmed the protrusion of

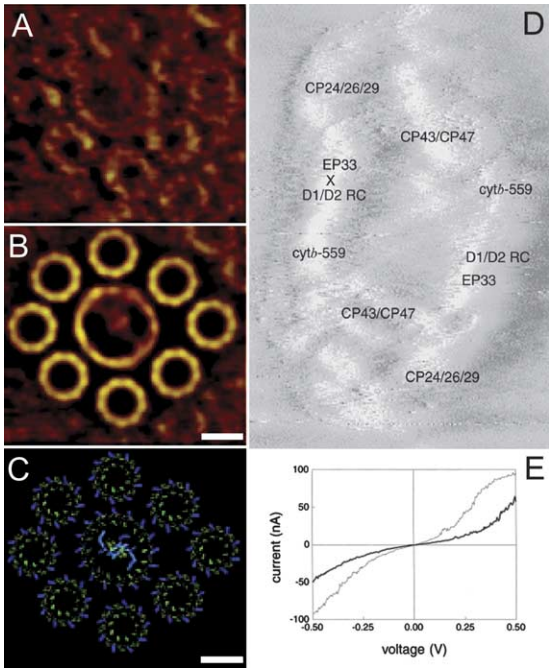

Fig. 6. High resolution images of photosynthetic pigment protein complexes. (A–C) Complexes of reaction centres (RC) associated with their inner (LH1) and outer (LH2) antennae complexes visualised by scanning force microscopy (SFM) in native membranes of purple bacteria *Rhodobacter sphaeroides* (Scheuring et al., 2004b). (A) Raw SFM image depicts a central RC-LH1 complex surrounded by eight LH2 complexes. Full colour range is 3 nm. (B) The topography of raw image fitted with the average structures of RC, LH1 and LH2. (C) Structure of individual units solved by X-ray crystallography fitted over the actual structure observed by SFM. Scale bar represents 5 nm. (D) Scanning tunnelling microscopy (STM) image of a Photosystem II complex (PSII) acquired at 1.5 nA tunnelling current and 0.2 V bias voltage. Individual pigment protein complexes of PSII are labelled (CP, chlorophyll proteins; D1/D2, proteins of the core of reaction centre; EP, extrinsic protein; cyt, cytochrome). The image size is 180×25 nm. (E) Plot of the tunnelling current measured in dark (thick line) and under white light (thin line) in a place designated with a cross in the D image (Lukins, 2000).

10±1 and 5±1 Å for the periplasmic and the cytoplasmic face of the *Rhodobacter sphaeroides* LH2 complexes by tapping mode in liquid. The overall organisation of RC–LH1–LH2 complex of *Rhodobacter sphaeroides* is shown in Fig. 6(A)–(C).

4.1.3. Light-harvesting chlorosomes of green bacteria

The light-harvesting of green photosynthetic bacteria relies on the self assembling rod elements of Bchl molecules enclosed by the monogalactosyl diglyceride monolayer. These supramolecular complexes adjacent to the inner surface of the cytoplasmatic membrane termed chlorosomes have been imaged in air by tapping and contact mode SFM albeit at low resolution. Zhu et al. (1995) imaged surface of carbon coated chlorosomes of *Chloroflexus aurantiacus* and report five-fold increase in chlorosome volume upon the 68 mM hexanol treatment and changes in the shape of 1% SDS treated chlorosome. Martinez-Planells et al. (2002) gave valuable biometry data on chlorosomes of five bacteria and provided solid evidence for the smooth surface of *Chloroflexus aurantiacus*, *Chloronema* sp. and *Chlorobium tepidum* chlorosomes contrasting with the rough one in *Chlorobium phaeobacteroides* and *Chlorobium vibrioforme*, probably due to the differences in the Csm peptide and glycolipid composition. Saga et al. (2002) characterised the sizes and spatial distribution of chlorosomes of *Chloroflexus aurantiacus* immobilised for the fluorescence emission spectroscopy. Montano et al. (2003) calculated value of 2,15,000±80,000 molecules of Bchl c present in the single chlorosome of *Chlorobium tepidum* based on the volume calculated from the SFM topography combined with the data from the fluorescence correlation spectroscopy.

4.1.4. Photosystem II (PSII)

To date, no high resolution topography obtained by SFM is available for the PSII supercomplex. Images obtained by contact mode SFM in air of PSII tubular crystals and grana membranes coated by 3.5 nm titanium are devoid of substructural details (Lyon et al., 1993). Shao et al. (1997) imaged spinach PSII in Langmuir–Blodgett films compressed to various pressures by tapping mode in air. Under the applied force of 300 pN, the PSII appear as blob-like, 250±50 Å wide particles protruding 5–25 Å above the lipid face. Upon increasing the applied force to 5 nN, the central cavity of the PSII particles become prominent, concomitant with the 10 Å compression of the face protruding above the membrane, signifying a PSII force constant of 5 nN nm^{-1}.

4.1.5. Photosystem I (PSI)

Fotiadis et al. (1998) imaged 2D crystals of PSI from thermophilic cyanobacterium *Synechococcus* sp. OD24 in contact mode SFM in liquid. The stromal and lumenal surfaces of PSI are imaged at high resolution, discerning the PsaC, D, E stromal side subunits including the estimation of their mass based on their volume. The tip loaded with a force of 100 pN sequentially removed the extrinsic stromal subunits revealing the underlying structural details of the PSI core. Similarly, PsaF, J were removed from the lumenal side. The details on the extramembranal loops of the PSI stroma exposed subunits of the former 4 Å resolution, X-ray diffraction based model are compared with the AFM images of the PSI.

4.1.6. Light-harvesting complex of photosystem II (LHCII)

The topography of the rye LHC II reconstituted in a monocomponent Langmuir–Blodgett film imaged by contact and tapping mode SFM under ambient conditions reveal structures corresponding to 50–140 monomers of LHC II organised in a ring like structure 300–500 Å in diameter. The potential to form such structures in the native membrane raises the possibility for interaction with PSII dimer and its incorporation at its centre, providing means to delocalisation and quenching of electronic excitation by thermal equilibration (Kernen et al., 1998). Gruszecki et al. (1999) showed 8% increase in surface area of the LB films containing the rye LHC II complexes imaged by tapping mode SFM in liquid upon temperature shift from 20 to 27 °C but the images lack the details that might give clues on the nature of the thermally induced conformational changes.

4.1.7. Membranes of purple photosynthetic bacteria

Scheuring et al. (2003a) imaged the individual complexes in *Rhodopseudomonas viridis* membranes but paid little attention to the apparent lateral heterogeneity of the RC–LH1 complexes. Bahatyrova et al. (2004b) report domains of linear arrays of the dimeric RC–LH1–PufX complexes including 10–20 LH2 complexes. These domains are interconnected by two to three LH2 complexes, but individual domains of large aggregates of LH2 also exist. Scheuring et al. (2004b) report the non-random lateral organisation of the RC–LH1 and LH2 complexes in native membranes of *Rhodospirillum photometricum*. The RC–LH1 domain hosts complexes clustered at high probability, with the RC–RC distances below 250 Å. Second domain is devoid of RC–LH1 complexes, where LH2 are packed in hexagonal lattices. Speculation arises that the empty spaces within the RC domain may host the cytochrome bc_1 that has been identified in the SDS/PAGE of the isolated membrane. The correlation function of the inter-complex distances shows a dominant 75 Å peak for the 2(LH2) in the hexagonal lattices. The RC–LH1 complex in direct contact with LH2 corresponds to the 95 Å peak, while the distance of 115 Å corresponds to the two RC–LH1 complexes in a direct contact. The 195 Å peak signifies a 2(RC–LH1)–LH2 complex, while the strong shoulder at 160 Å comes from a pair of LH2 sandwiched between the two RC–LH1 complexes.

4.1.8. Thylakoid membranes and whole chloroplasts

The native photosynthetic membranes were among the first biological samples that were imaged with SFM,

although at low resolution (Azumi et al., 1991). Highly resolved topography of whole intact de-enveloped chloroplasts were visualised only recently. Kaftan et al. (2002) imaged the native and glutaraldehyde fixed lettuce chloroplasts by contact and tapping mode in air. Individual protein complexes identified over the thylakoid surface were classified according to the apparent shape and dimensions of their extramembranous protrusions. PSI was identified as a dominant component of the grana margins based on the membrane topography and confirmed by tapping mode SFM in air of the chloroplasts immunologically labelled against the PSI and ATP synthase. Dynamics of the reversible grana unstacking was assessed in non-fixed chloroplasts. More recent efforts include low resolution imaging of spinach thylakoids. Liou et al. (2002) used contact mode SFM in liquid to create calibrated differential electrostatic measurements for the time resolved phosphorylation maps of PSII enriched thylakoid membranes, reporting densities of 0.044 ± 0.005 P_i nm^{-2}. Gradinaru et al. (2004) monitored thylakoids under process of destacking by tapping mode SFM in air paralleled by laser two photon confocal microscopy. Kirchhoff et al. (2004) imaged height steps of the stacked grana membrane and showed individual PSII particles in the destacked thylakoids by tapping mode SFM in air.

4.2. Scanning tunnelling microscopy

The fundamental design of the STM includes a sharp metallic probe that is being raster scanned within a distance of few angstroms above a conductive sample. This small distance allows for an effective overlap of the wavefunctions of the tip and the sample. As a result, the tunnelling current of ~ 1 nA is measured between the sample and the tip under the applied bias DC voltage (1–2 V). The inherent high sensitivity of the STM is due the tunnelling current depending quadratically on a probability density for the wavefunctions on both sides of the tunnelling gap and, exponentially on the separation distance. The STM image of a conductive material thus reveals the surface topography along with the electronic density of states of the sample at Å lateral and sub Å vertical resolution. The technique's ability to produce faithful, reproducible images of large, non-conducting macromolecules is somewhat limited, although smaller molecules have been imaged in vacuum or at solid–liquid interface at or near atomic resolution (reviewed in Ikai, 1996).

The STM studies of the photosynthetic reaction centres and the light-harvesting complexes have been often limited by the requirement for the semidry samples to be scanned under ambient conditions. The low conductance of the imaged specimens often results in apparent topography heights that are ca. one order of magnitude lower than expected. That is why the STM never really attained, the high-resolution topographies seen in SFM studies. Nevertheless, accurate measurements of the voltage–current (*I–V*) curves at high spatial resolution are possible. These measurements are mostly concerned with distinct changes in the conductivity of the reaction centres and light-harvesting complexes under light to dark transition.

4.2.1. Bacterial reaction centres (RC)

The early *I–V* measurements on individual *Rhodobacter sphaeroides* RC complexes by Alekperov et al. (1989) suggest the presence of a large electric dipole moment. Facci et al. (1994) measured highly asymmetric *I–V* curves of the RC from *Rhodobacter sphaeroides* reconstituted in LB films. A dominant resonance at a tip-substrate voltage of 3.16 V appeared in the dark whereas no measurable resonance was detected under 100 W illumination, that turns the RC in an apparently permanent dipole. The dark-light transition led to a remarkable change in surface potentials, that stand 20 ± 1 and 344 ± 1 mV for the RC imaged in dark and light, respectively. The *I–V* curves for the *Rhodopseudomonas sphaeroides* RC reconstituted in a lipid bilayer were also highly asymmetric (Stamouli et al., 2004). In the RC facing with the cytoplasmic side toward the scanning tip, electron transfer has increased in reverse bias and remained small in a forward bias. This asymmetry is being related to the disproportionate forward and backward electron transfer within the native RC.

4.2.2. Bacterial light-harvesting complex (LH2)

The highly symmetric *I–V* curves of the reconstituted LH2 complexes from *Rhodopseudomonas acidophila* (Stamouli et al., 2004) were centred at about 0 V. While the large distance of the supporting surface to bacteriochlorophyll molecules rules out their involvement in the electron transfer pathway, carotenoids, which are present within the LH2 structure, may potentially play a role in the electron conduction.

4.2.3. Photosystem II (PSII)

The spinach PS II membrane fragments and PS II core complexes were imaged at a 3–4 Å resolution, that allowed Lukins and Oates (1998) to assign the individual protein subunits in the 301×125 Å BBY particles and the 189×94 Å PS II complexes ($90 \pm 7\%$ were PS II dimmers), despite the erroneous estimations of the sample height (Fig. 6(D)). Contrary to the bacterial RC, the PS II *I–V* curves were symmetrical at about $V = 0$. In dark, the D1/D2 area of the PS II has a diode-like behaviour with an effective band-gap of 0.4 eV and an unusually high maximum local density of states near its surface. Under while light, photoconduction dramatically increases between -1 and $+1$ V but shows no change outside this voltage range (Fig. 6(E)). The detailed model of the conductivity and photovoltaic behaviour of a single PS II was proposed by Lukins (2000), relating the energy vibronic bands to the actual structural elements of the RC. In summary, the RC acts as a parallel combination of an ideal semiconductor junction, shunt permanent impedance and delocalised

conduction. Recently, Lukins and Barton (2003) also observed localised spatially-coherent electron tunnelling through single complexes in PS II 2D crystal.

4.2.4. Photosystem I (PSI)

Lee et al. (1995) show images of bare ($60\times50\pm1$ Å, 4 Å height) and lightly platinised ($90\times70\pm1$ Å, 5 Å height) spinach PS I immobilised on gold functionalised by mercaptoacetic acid. The low height of the particles is being explained by the very high gap resistance. The *I–V* curve of the bare PS I has a band gap of 1.8 eV that is symmetric at 0 V while the lightly platinised PS I behave as an n-type doped semiconductor. The *I–V* curves of the PS I absorbed to the functionalised gold surfaces provide evidence for the sidedness of the PS I complex under differing adsorbing conditions (Lee et al., 1997).

4.2.5. Light-harvesting complex of photosystem II (LHCII)

The LHC II complexes that are adjacent to the spinach PSII complex were imaged at 4 Å resolution by Lukins (1999). The light activation results in an increase in the delocalisation of the electrons, but the overall effect is rather photoconductive than photovoltaic. No evidence is found for the diode-like behaviour found earlier in the RC.

4.2.6. Whole photosynthetic membranes

The STM images of the membrane fragments isolated from *Rhodospirillum rubrum* reveal two distinct domains illustrating the intrinsic heterogeneity of the native membranes. Regions of ordered, densely packed particles dominated the membranes, while hexagonally packed particles spaced by 40 Å populated minor but distinct areas. The *I–V* curves measured selectively on the ordered polypeptide structure have an asymmetric shape (Golubok et al., 1992).

Mainsbridge and Thundat (1991) imaged grana and stroma lamellae of spinach chloroplasts. Low resolution images of gold-coated chloroplasts in air and bare chloroplasts in solution were provided by Dahn et al. (1992) including the structure on the chloroplast outer membrane.

Acknowledgements

This work was supported by grants (FV) MSM6007665808, (LB) AV0Z50510513 and (DK) AV0Z60870520.

References

Adrian, M., Dubochet, J., Fuller, S.D., Harris, J.R., 1998. Cryo-negative staining. Micron 29, 145–160.

Alekperov, S.D., Vasiljev, S.I., Kononenko, A.A., Lukashev, E.P., Panov, V.I., Semenov, A.E., 1989. Scanning tunneling microscopy of photosynthetic reaction centers. Chemical Physics Letters 164 (2-3), 151–154.

Azoulay, J., Debarre, A., Jaffiol, R., Tchenio, P., 2001. Original tools for single molecule spectroscopy. Single Molecules 2, 241–249.

Azumi, R., Matsumoto, M., Kawabata, Y., Ichimura, T., Mizuno, T., Miyamoto, H., 1991. Atomic force microscopic study of vesicles of synthetic surfactant, vesicles of thylakoid membrane, and whole cells of bacteria. Chemistry Letters 11, 1925–1928.

Bahatyrova, S., Frese, R.N., Siebert, C.A., Olsen, J.D., van der Werf, K.O., van Grondelle, R., Niederman, R.A., Bullough, P.A., Otto, C., Hunter, C.N., 2004a. The native architecture of a photosynthetic membrane. Nature 430 (7003), 1058–1062.

Bahatyrova, S., Frese, R.N., van der Werf, K.O., Cees, O., Hunter, C.N., Olsen, J.D., 2004b. Flexibility and size heterogeneity of the LH1 light-harvesting complex revealed by atomic force microscopy—functional significance for bacterial photosynthesis. Journal of Biological Chemistry 279 (20), 21327–21333.

Barber, J., Andersson, B., 1992. Too much of a good thing—light can be bad for photosynthesis. Trends in Biochemical Sciences 17, 61–66.

Bartko, A., Dickson, R.M., 1999. Imaging three-dimensional single molecule orientations. Journal of Physical Chemistry B 103, 11237–11241.

Bassi, R., Magaldi, A.G., Tognon, G., Giacometti, G.M., Miller, K.R., 1989. Two-dimensional crystals of the photosystem II reaction center complex from higher plants. European Journal of Cell Biology 50, 84–93.

Ben-Shem, A., Frolow, F., Nelson, N., 2003. Crystal structure of plant photosystem I. Nature 426, 630–635.

Best, R.B., Brockwell, D.J., Toca-Herrera, J.L., 2003. Force mode atomic force microscopy as a tool for protein folding studies. Analytica Chimica Acta 479 (1), 87–105.

Betzig, E., Chichester, R.J., 1993. Single molecules observed by near-field scanning optical microscopy. Science 262, 1422–1425.

Bibby, T.S., Nield, J., Barber, J., 2001a. Iron deficiency induces the formation of an antenna ring around trimeric photosystem I in cyanobacteria. Nature 412, 743–745.

Bibby, T.S., Nield, J., Partensky, F., Barber, J., 2001b. Oxyphotobacteria-antenna ring around photosystem I. Nature 413, 590.

Bibby, T.S., Nield, J., Chen, M., Larkum, A.W.D., Barber, J., 2003. Structure of a photosystem II supercomplex isolated from *Prochlorion didemni* retaining its chlorophyll a/b light-harvesting system. Proceedings of the National Academy of Sciences of USA 100 pp. 9050–9054.

Binnig, G., Rohrer, H., Gerber, C., Weibel, E., 1982. Surface studies by scanning tunnelling microscopy. Physical Review Letter 49, 57–61.

Binnig, G., Quate, C.F., Gerber, C., 1986. Atomic force microscope. Physical Review Letter 56, 930–933.

Boekema, E.J., 1991. Negative staining of integral membrane proteins. Micron and Microscopica Acta 22, 361–369.

Boekema, E.J., Dekker, J.P., van Heel, M.G., Rogner, M., Saenger, W., Witt, I., Witt, H.T., 1987. Evidence for a trimeric organization of the Photosystem I complex from the thermophilic cyanobacterium Synechococcus sp. FEBS Letters 217, 283–286.

Boekema, E.J., Wynn, R.M., Malkin, R., 1990. The structure of spinach Photosystem I studied by electron microscopy. Biochimica et Biophysica Acta 1017, 49–56.

Boekema, E.J., Hankamer, B., Bald, D., Kruip, J., Nield, J., Boonstra, A.F., Barber, J., Rogner, M., 1995. Supramolecular structure of the photosystem II complex from green plants and cyanobacteria. Proceedings of the National Academy of Sciences of the United States of America 92, 175–179.

Boekema, E.J., Nield, J., Hankamer, B., Barber, J., 1998a. Localization of the 23-kDa subunit of the oxygen evolving complex of photosystem II by electron-microscopy. European Journal of Biochemistry 252, 268–276.

Boekema, E.J., van Roon, H., Dekker, J.P., 1998b. Specific association of photosystem II and light-harvesting complex II in partially solubilized photosystem II membranes. FEBS Letters 424, 95–99.

Boekema, E.J., van Roon, H., Calkoen, F., Bassi, R., Dekker, J.P., 1999a. Multiple types of association of photosystem II and its light-harvesting antenna in partially solubilized photosystem II membranes. Biochemistry 38, 2233–2239.

Boekema, E.J., van Roon, H., van Breemen, J.F.L., Dekker, J.P., 1999b. Supramolecular organization of photosystem II and its light-harvesting antenna in partially solubilized photosystem II membranes. European Journal of Biochemistry 266, 444–452.

Boekema, E.J., van Breemen, J.F.L., van Roon, H., Dekker, J.P., 2000a. Arrangement of photosystem II supercomplexes in crystalline macrodomains within the thylakoid membrane of green plant chloroplasts. Journal of Molecular Biology 301, 1123–1133.

Boekema, E.J., van Breemen, J.F.L., van Roon, H., Dekker, J.P., 2000b. Conformational changes in photosystem II supercomplexes upon removal of extrinsic subunits. Biochemistry 39, 12907–12915.

Boekema, E.J., Jensen, P.E., Schlodder, E., van Breemen, J.F.L., van Roon, H., Scheller, H.V., Dekker, J.P., 2001a. Green plant photosystem I binds light-harvesting complex I on one side of the complex. Biochemistry 40, 1029–1036.

Boekema, E.J., Hifney, A., Yakushevska, A.E., Piotrowski, M., Keegstra, W., Berry, S., Michel, K.P., Pistorius, E.K., Kruip, J., 2001b. A giant chlorophyll–protein complex induced by iron deficiency in cyanobacteria. Nature 412, 745–748.

Bopp, M.A., Jia, Y., Li, L., Cogdell, R.J., Hochstrasser, R.M., 1997. Fluorescence and photobleaching dynamics of single light-harvesting complexes. Proceeding of the National Academy of Sciences USA 94, 10630–10635.

Bopp, M.A., Sytnik, A., Howard, T.D., Cogdell, R.J., Hochstrasser, R.M., 1999. The dynamics of structural deformations of immobilized single light-harvesting complexes. Proceeding of the National Academy of Sciences USA 96, 11271–11276.

Böttcher, B., Graber, P., Boekema, E.J., 1992. The structure of photosystem I from the thermophilic cyanobacterium Synechococcus sp. determined by electron microscopy of 2-D crystals. Biochimica et Biophysica Acta 1100, 125–136.

Braga, P.C., Ricci, D., 2003. Atomic Force Microscopy: Biomedical Methods and Applications, Methods in Molecular Biology 242. Humana Press, New Jersey.

Bumba, L., Vácha, F., 2003. Electron microscopy in structural studies of Photosystem II. Photosynthesis Research 77, 1–19.

Bumba, L., Havelkova-Dousova, H., Husak, M., Vacha, F., 2004a. Structural characterization of Photosystem II complex from red alga *Porphyridium cruentum* retaining extrinsic subunits of the oxygen-evolving complex. European Journal of Biochemistry 271, 2967–2975.

Bumba, L., Husak, M., Vacha, F., 2004b. Interaction of PSII–LHCII supercomplexes in adjacent layers of stacked chloroplast thylakoid membranes. Photosynthetica 42, 193–199.

Bumba, L., Prasil, O., Vacha, F., in press. Antenna ring around trimeric photosystem I in chlorophyll b containing cyanobacterium *Prochlorothrix hollandica*. Biochimica et Biophysica Acta.

Büchel, C., Morris, E., Orlova, E., Barber, J., 2001. Localization of the PsbH subunit in photosystem II. A new approach using labeling of His-tags with a Ni^{2+}-NTA gold cluster and single particle analysis. Journal of Molecular Biology 312, 371–379.

Cogdell, R.J., Gardiner, A.T., Roszak, A.W., Law, C.L., Southall, J., Isaacs, N.W., 2004. Rings, ellipses and horseshoes: how purple bacteria harvest solar energy. Photosynthetic Research 81 (3), 207–214.

Dahn, D.C., Cake, K., Hale, L.R., 1992. Scanning tunnelling microscopy of unbroken chloroplasts. Ultramicroscopy 42–44, 1222–1227.

Dekker, J.P., Boekema, E.J., Witt, H.T., Rogner, M., 1988. Refined purification and further characterization of oxygen-evolving and Tris-treated photosystem II particles from the thermophilic cyanobacterium Synechococcus sp. Biochimica et Biophysica Acta 936, 307–318.

Dekker, J.P., Betts, S.D., Yocum, C.F., Boekema, E.J., 1990. Characterization by electron microscopy of isolated particles and two-dimensional crystals of the CP47-D1-D2-cytochrome b_{559} complex of photosystem II. Biochemistry 29, 3220–3225.

Dunn, R.C., Holtom, G.R., Mets, L., Xie, X.S., 1994. Near-field fluorescence imaging and fluorescence lifetime measurement of light-harvesting complexes in intact photosynthetic membranes. Journal of Physical Chemistry 98, 3094–3098.

Empedocles, S.A., Neuhauser, R., Bawendi, M.G., 1999. Three-dimensional orientation measurements of symmetric single chromophores using polarization microscopy. Nature 399, 126–130.

Facci, P., Erokhin, V., Nicolini, C., 1994. Scanning tunnelling microscopy of a monolayer of reaction centres. Thin Solid Films 243, 403–406.

Ferreira, K.N., Iverson, T.M., Maghlaoui, K., Barber, J., Iwata, S., 2004. Architecture of the photosynthetic oxygen-evolving center. Science 303, 1831–1838.

Ford, R.C., Holzenburg, A., 1988. Investigation of the structure of trimeric and monomeric Photosystem I reaction center complex. EMBO Journal 7, 2287–2293.

Ford, R.C., Hefti, A., Engel, A., 1990. Ordered arrays of the photosystem I reaction center after reconstitution-projections and surface reliefs of the complex at 2-nm resolution. EMBO Journal 9, 3067–3075.

Ford, R.C., Rosenberg, M.F., Shepherd, F.H., McPhie, P., Holzenburg, A., 1995. Photosystem II 3-D structure and the role of the extrinsic subunits in photosynthetic oxygen evolution. Micron 26, 133–140.

Ford, R.C., Stoylova, S.S., Holzenburg, A., 2002. An alternative model for photosystem II/light-harvesting complex II in grana membranes based on cryo-electron microscopy studies. European Journal of Biochemistry 269, 326–336.

Forkey, J.N., Quinlan, M.E., Shaw, M.A., Corrie, J.E., Goldman, Y.E., 2003. Three-dimensional structural dynamics of myosin V by single-molecule fluorescence polarization. Nature 422, 399–404.

Fotiadis, D., Muller, D.J., Tsiotis, G., Hasler, L., Tittmann, P., Mini, T., Jeno, P., Gross, H., Engel, A., 1998. Surface analysis of the photosystem I complex by electron and atomic force microscopy. Journal of Molecular Biology 283, 83–94.

Fotiadis, D., Scheuring, S., Muller, S.A., Engel, A., Muller, D.J., 2002. Imaging and manipulation of biological structures with the AFM. Micron 33, 385–397.

Fotiadis, D., Qian, P., Pilippsen, A., Bullough, P.A., Engel, A., Hunter, C.N., 2004. Structural analysis of the reaction center light-harvesting complex I photosynthetic core complex of *Rhodospirillum rubrum* using atomic force microscopy. Journal of Biological Chemistry 279, 2063–2068.

Fourkas, J.T., 2001. Rapid determination of the three-dimensional orientation of single molecules. Optics Letters 26, 211–213.

Frank, J., 2002. Single-particle imaging of macromolecules by cryo-electron microscopy. Annual Review of Biophysics and Biomolecular Structure 31, 303–319.

Garcia, R., Perez, R., 2002. Dynamic atomic force microscopy methods. Surface Science Reports 47 (6-8), 197–301.

Germano, M., Yakushevska, A.E., Keegstra, W., van Gorkom, H.J., Dekker, J.P., Boekema, E.J., 2002. Supramolecular organization of photosystem I and light-harvesting complex I in Chlamydomonas reinhardtii. FEBS Letters 525, 121–125.

Gerken, U., Wolf-Klein, H., Huschenbett, C., Goetze, B., Schuler, S., Jelezko, F., Tietz, C., Wrachtrup, J., Paulsen, H., 2002. Single molecule spectroscopy of oriented recombinant trimeric light harvesting complexes of higher plants. Single Molecules 3, 183–188.

Gerken, U., Jelezko, F., Goetze, B., Branschaedel, M., Tietz, C., Ghosh, R., Wrachtrup, J., 2003a. Membrane environment reduces the accessible conformational space to an integral membrane protein. Journal of Physical Chemistry B 107, 338–343.

Gerken, U., Lupo, D., Tietz, C., Wrachtrup, J., Ghosh, R., 2003b. Circular symmetry of the light-harvesting 1 complex from *Rhodospirillum rubrum* is not perturbed by interaction with the reaction center. Biochemistry 42, 10354–10360.

Golubok, A.O., Vinogradova, S.A., Tipisev, S.Y., Borisov, A.Y., Taisova, A.S., Kolomytkin, O.V., 1992. STM/STS study of photosynthetic bacterial membrane. Ultramicroscopy 42–44, 1228–1235.

Gordon, M.P., Ha, T., Selvin, P.R., 2004. Single-molecule high-resolution imaging with photobleaching. Proceeding of the National Academy of Sciences USA 101, 6462–6465.

Green, B.R., Durnford, D.G., 1996. The chlorophyll-carotenoid proteins of oxygenic photosynthesis. Annual Review of Plant Physiology and Plant Molecular Biology 47, 685–714.

Gradinaru, C.C., Martinsson, P., Aartsma, T.J., Schmidt, T., 2004. Simultaneous atomic-force and two-photon fluorescence imaging of biological specimens in vivo. Ultramicroscopy 99 (4), 235–245.

Grigorieff, N., 1998. Three-dimensional structure of bovine NADH, ubiquinone oxidoreductase, complex I. at 22 Å in ice. Journal of Molecular Biology 277, 1033–1046.

Grigorieff, N., Ceska, T.A., Downing, K.H., Baldwin, J.M., Henderson, R., 1996. Electron-crystallographic refinement of the structure of bacteriorhodopsin. Journal of Molecular Biology 259, 393–421.

Gruszecki, W.I., Grudzinski, W., Matula, M., Kernen, P., Krupa, Z., 1999. Light-induced excitation quenching and structural transition in light-harvesting complex II. Photosynthesis Research 59 (2-3), 175–185.

Gunning, B.E.S., Schwartz, O.M., 1999. Confocal microscopy of thylakoid autofluorescence in relation to origin of grana and phylogeny in the green algae. Australian Journal of Plant Physiology 26, 695–708.

Hankamer, B., Boekema, E.J., Barber, J., 1997. Structure and membrane organization of photosystem II in green plants. Annual Review of Plant Physiology and Plant Molecular Biology 48, 641–671.

Hankamer, B., Morris, E.P., Nield, J., Gerle, C., Barber, J., 2001. Three-dimensional structure of the Photosystem II core dimer of higher plants determined by electron microscopy. Journal of Structural Biology 135, 262–269.

Harris, J.R., Scheffler, D., 2002. Routine preparation of air-dried negatively stained and unstained specimens on holey carbon support films, a review of applications. Micron 33, 461–480.

Henderson, R., 2004. Realizing the potential of electron cryo-microscopy. Quarterly Review of Biophysics 37, 3–13.

Henderson, R., Baldwin, J.M., Ceska, T.A., Zemlin, F., Beckmann, E., Downing, K.H., 1990. Model for the structure of bacteriorhodopsin based on high-resolution electron cryomicroscopy. Journal of Molecular Biology 213, 899–929.

Hepler, P.K., Gunning, B.E.S., 1998. Confocal fluorescence microscopy of plant cells. Protoplasma 201, 121–157.

Heymann, J.B., Cheng, N., Newcomb, W.W., Trus, B.L., Brown, J.C., Steven, A.C., 2003. Dynamics of herpes simplex virus capsid maturation visualized by time-lapse cryo-electron microscopy. Nature Structural Biology 10, 334–341.

Hofmann, C., Ketelaars, M., Matsushita, M., Michel, H., Aartsma, T.J., Koehler, J., 2003a. Single-molecule study of the electronic coupling in a circular array of molecules: light-harvesting-2 complex from *Rhodospirillum molischianum*. Physical Review Letters 90. Art. No. 0130004.

Hofmann, C., Aartsma, T.J., Michel, H., Koehler, J., 2003b. Direct observation of tiers in the energy landscape of a chromoprotein: a single-molecule study. Proceeding of the National Academy of Sciences USA 100, 15534–15538.

Hofmann, C., Francia, F., Venturoli, G., Oesterhelt, D., Koehler, J., 2003c. Energy transfer in a single self-aggregated photosynthetic unit. FEBS Letters 546, 345–348.

Ikai, A., 1996. STM and AFM in bio/organic molecules and structures. Surface Science Reports 26, 261–332.

Jelezko, F., Tietz, C., Gerken, U., Wrachtrup, J., Bittl, R., 2000. Single molecule spectroscopy on Photosystem I pigment–protein complexes. Journal of Physical Chemistry B 104, 8093–8096.

Jordan, P., Fromme, P., Witt, H.T., Klukas, O., Saenger, W., Krauss, N., 2001. Three-dimensional structure of cyanobacterial photosystem I at 2.5 Å resolution. Nature 411, 909–917.

Kaftan, D., Brumfeld, V., Nevo, R., Scherz, A., Reich, Z., 2002. From chloroplast to photosystems: in situ scanning force microscopy on intact thylakoid membranes. EMBO Journal 21, 6146–6153.

Kamiya, N., Shen, J.R., 2003. Crystal structure of oxygen-evolving Photosystem II from Thermosynechococcus vulcanus at 3.7 Å resolution. Proceedings of the National Academy of Sciences of the United States of America 100, 98–103.

Kargul, J., Nield, J., Barber, J., 2003. Three-dimensional reconstruction of a light-harvesting complex I-photosystem I, LHCI–PSI supercomplex from the green alga *Chlamydomonas reinhardtii*—insights into light harvesting for PSI. Journal of Biological Chemistry 278, 16135–16141.

Karrasch, S., Typke, D., Walz, T., Miller, M., Tsiotis, G., Engel, A., 1996. Highly ordered two-dimensional crystals of photosystem I reaction center from Synechococcus sp. Functional and structural analyses. Journal of Molecular Biology 262, 336–348.

Kernen, P., Gruszecki, W.I., Matula, M., Wagner, P., Ziegler, U., Krupa, Z., 1998. Light-harvesting complex II in monocomponent and mixed lipid–protein monolayers. Biochimica et Biophysica Acta Biomembranes 1373 (2), 289–298.

Ketelaars, M., van Oijen, A.M., Matsushita, M., Koehler, J., Schmidt, J., Aartsma, T.J., 2001. Spectroscopy on the B850 band of individual ligh-harvesting 2 complexes of *Rhodopseudomonas acidophila* I. Experiments and Monte Carlo simulations. Biophysical Journal 80, 1591–1603.

Ketelaars, M., Hofmann, C., Koehler, J., Howard, T.D., Cogdell, R.J., Schmidt, J., Aartsma, T.J., 2002. Spectroscopy on individual light-harvesting 1 complexes of *Rhodopseudomonas acidophila*. Biophysical Journal 83, 1701–1715.

Kirchhoff, H., Borinski, M., Lenhert, S., Chi, L., Buechel, C., 2004. Transversal and lateral exciton energy transfer in grana thylakoids of spinach. Biochemistry 43, 14508–14516.

Kitmitto, A., Mustafa, A.O., Holzenburg, A., Ford, R.C., 1998. Three-dimensional structure of higher plant photosystem I determined by electron crystallography. Journal of Biological Chemistry 273, 29592–29599.

Krauss, N., Hinrichs, W., Witt, I., Fromme, P., Pritzkow, W., Dauter, Z., Betzel, C., Wilson, K.S., Witt, H.T., Saenger, W., 1993. 3-Dimensional structure of photosystem I of photosynthesis at 6 angstrom resolution. Nature 361, 326–331.

Kruip, J., Boekema, E.J., Bald, D., Boonstra, A.F., Rogner, M., 1993. Isolation and structural characterization of monomeric and trimeric Photosystem I complexes, P700*FA/FB and P700*FX from the cyanobacterium Synechocystis PCC 6803. Journal of Biological Chemistry 268, 23353–23360.

Kruip, J., Chitnis, P.R., Lagoutte, B., Rogner, M., Boekema, E.J., 1997. Structural organization of the major subunits in cyanobacterial photosystem I—localization of subunits PsaC,-D,-E,-F, and-. J. Journal of Biological Chemistry 272, 17061–17069.

Kuhl, H., Rogner, M., van Breemen, J.F.L., Boekema, E.J., 1999. Localization of cyanobacterial photosystem II donor-side subunits by electron microscopy and the supramolecular organization of photosystem II in the thylakoid membrane. European Journal of Biochemistry 266, 453–459.

Kühlbrandt, W., 1992. 2-Dimensional crystallization of membrane proteins. Quarterly Review of Biophysics 25, 1–49.

Kühlbrandt, W., Wang, D.N., Fujiyoshi, Y., 1994. Atomic model of plant light-harvesting complex by electron crystallography. Nature 367, 614–621.

Kulzer, F., Orrit, M., 2004. Single molecule optics. Annual Review of Physical Chemistry 55, 585–611.

Lee, I., Lee, J.W., Warmack, R.J., Allison, D.P., Greenbaum, E., 1995. Molecular electronics of a single photosystem I reaction center: studies with scanning tunnelling microscopy and spectroscopy. Proceedings of the National Academy of Sciences of the United States of America 92, 1965–1969.

Lee, I., Lee, J.W., Greenbaum, E., 1997. Biomolecular electronics: vectorial arrays of photosynthetic reaction centers. Physical Review Letter 79, 3294–3297.

Lee, I., Lee, J.W., Stubna, A., Greenbaum, E., 2000. Measurement of electrostatic potentials above oriented single photosynthetic reaction centers. Journal of Physical Chemistry B 104, 2439–2443.

Lieb, M.A., Zavislan, J.M., Novotny, L., 2004. Single-molecule orientations determined by direct emission pattern imaging. Journal of the Optical Society of America B 21, 1210–1215.

Liou, J.W., Mulet, X., Klug, D.R., 2002. Absolute measurement of phosphorylation levels in a biological membrane using atomic force microscopy: the creation of phosphorylation maps. Biochemistry 41 (27), 8535–8539.

Liu, Z.F., Yan, H.C., Wang, K.B., Kuang, T.Y., Zhang, J.P., Gui, L.L., An, X.M., Chang, W.R., 2004. Crystal structure of spinach major light-harvesting complex at 2.72 angstrom resolution. Nature 428, 287–292.

Lukins, P.B., 1999. Single-molecule electron tunnelling spectroscopy of the higher plant light-harvesting complex LHC II. Biochemical and Biophysical Research Communications 256 (2), 288–292.

Lukins, P.B., 2000. Direct observation of semiconduction and photovoltaic behaviour in single molecules of the photosystem II reaction centre. Chemical Physics Letters 321, 13–20.

Lukins, P.B., Oates, T., 1998. Single-molecule high-resolution structure and electron conduction of photosystem II from scanning tunnelling microscopy and spectroscopy. Biochimica et Biophysica Acta 1409, 1–11.

Lukins, P.B., Barton, C.S., 2003. Evidence for spatially-coherent trans-molecular electron tunnelling through two-dimensional arrays of Photosystem II core complexes. Chemical Comminications 5, 602–603.

Lyon, M.K., 1998. Multiple crystal types reveal photosystem II to be a dimer. Biochimica et Biophysica Acta 1364, 403–419.

Lyon, M.K., Marr, K.M., Furcinitti, P.S., 1993. Formation and characterization of two-dimensional crystals of photosystem II. Journal of Structural Biology 110, 133–140.

Mainsbridge, B., Thundat, T., 1991. Scanning tunneling microscopy of chloroplasts. Journal of Vacuum Science and Technology B: Microelectronics and Nanometer Structures 9 (2), 1259–1262.

Marr, K.M., McFeeters, R.L., Lyon, M.K., 1996. Isolation and structural analysis of two-dimensional crystals of photosystem II from Hordeum vulgare viridis zb^{63}. Journal of Structural Biology 117, 86–98.

Martinez-Planells, A., Arellano, J.B., Borrego, C.A., Lopez-Iglesias, C., Gich, F., Garcia-Gil, J.S., 2002. Determination of the topography and biometry of chlorosomes by atomic force microscopy. Photosynthesis Research 71, 83–90.

Mayanagi, K., Ishikawa, T., Toyoshima, C., Inoue, Y., Nakazato, K., 1998. Three-dimensional electron microscopy of the photosystem II core complex. Journal of Structural Biology 123, 211–224.

Mehta, M., Sarafis, V., Critchley, C.C., 1999. Thylakoid membrane architecture. Australian Journal of Plant Physiology 26, 709–716.

Montano, G.A., Bowen, B.P., LaBelle, J.T., Woodbury, N.W., 2003. Characterization of *Chlorobium tepidum* chlorosomes: a calculation of bacteriochlorophyll c per chlorosome and oligomer modeling. Biophysical Journal 85 (4), 2560–2565.

Moreno-Herrero, F., Colchero, J., Gomez-Herrero, J., 2004. Atomic force microscopy contact, tapping, and jumping modes for imaging biological samples in liquids. Physical Review E 69 (3), 031915.

Mosser, G., 2001. Two-dimensional crystallogenesis of transmembrane proteins. Micron 32, 517–540.

Mueller, D.J., Janovjak, H., Lehto, T., Kuerschner, L., Anderson, K., 2002. Observing structure, function and assembly of single proteins by AFM. Progress in Biophysics and Molecular Biology 79, 1–43.

Myhra, S., 2004. A review of enabling technologies based on scanning probe microscopy relevant to bioanalysis. Biosensors and Bioelectronics 19 (11), 1345–1354.

Newman, P.J., Sherman, L.A., 1978. Isolation and characterization of Photosystem I and II membrane particles from the blue-green alga. Synechococcus cedorum. Biochimica et Biophysica Acta 503, 343–361.

Nield, J., Orlova, E.V., Morris, E.P., Gowen, B., van Heel, M., Barber, J., 2000. 3D map of the plant photosystem II supercomplex obtained by cryoelectron microscopy and single particle analysis. Nature Structural Biology 7, 44–47.

Nonnenmacher, M., O'Boyle, M.P., Wickramasinghe, H.K., 1991. Kelvin probe force microscopy. Applied Physics Letters 58 (25), 2921–2923.

Novotny, L., Beversluis, M.R., Youngworth, K.S., Brown, T.G., 2001. Longitudinal field modes probed by single molecules. Physical Review Letters 86, 5251–5254.

Osmond, B., Schwartz, O., Gunning, B., 1999. Photoinhibitory printing on leaves, visualised by chlorophyll fluorescence imaging and confocal microscopy, is due to diminished fluorescence from grana. Australian Journal of Plant Physiology 26, 717–724.

Pohl, D.W., Fischer, U.C., Durig, U.T., 1988. Scanning near field optical microscopy (SNOM). Journal of Microscopy 152, 853–861.

Pfundel, E., Neubohn, B., 1999. Assessing photosystem I and II distribution in leaves from C-4 plants using confocal laser scanning microscopy. Plant Cell and Environment 22, 1569–1577.

Prummer, M., Sick, B., Hecht, B., Wild, U.P., 2003. Three-dimensional optical tomography of single molecules. Journal of Chemical Physics 118, 9824–9829.

Psencik, J., Ikonen, T.P., Laurinmaki, P., Merckel, M.C., Butcher, S.J., Serimaa, R.E., Tuma, R., 2004. Lamellar organization of pigments in chlorosomes, the light harvesting complexes of green photosynthetic bacteria. Biophysical Journal 87, 1165–1172.

Qu, X., Wu, D., Mets, L., Scherer, N.F., 2004. Nanometer-localized multiple single-molecule fluorescence microscopy. Proceeding of the National Academy of Sciences USA 101, 11298–11303.

Rhee, K.H., Morris, E.P., Barber, J., Kühlbrandt, W., 1998. Three-dimensional structure of the plant photosystem II reaction centre at 8 Å resolution. Nature 396, 283–286.

Rigaud, J.L., Chami, M., Lambert, O., Levy, D., Ranck, J.L., 2000. Use of detergents in two-dimensional crystallization of membrane proteins. Biochimica et Biophysica Acta 1508, 112–128.

Rögner, M., Muhlenhoff, U., Boekema, E.J., Witt, H.T., 1990. Monomeric, dimeric and trimeric PSI reaction center complex isolated from the thermophilic cyanobacterium Synechococcus sp.—size, shape and activity. Biochimica et Biophysica Acta 1015, 415–424.

Roseman, A.M., 2000. Docking structures of domains into maps from cryo-electron microscopy using local correlation. Acta Crystallographica D 56, 1332–1340.

Roszak, A.W., Howard, T.D., Southall, J., Gardiner, A.T., Law, C.J., Isaacs, N.W., Cogdell, R.J., 2003. Crystal structure of RC–LH1 core complex from *Rhodopseudomonas palustris*. Science 302, 1969–1972.

Rousso, I., Khatchatryan, E., Brodsky, I., Nechustai, R., Ottolenghi, M., Sheves, M., Lewis, A., 1997. Atomic force sensing of light-induced protein dynamics with microsecod time resolution in bacteriorhodopsin and photosynthetic reaction centers. Journal of Structural Biology 119, 158–164.

Ruffle, S.V., Mustafa, A.O., Kitmitto, A., Holzenburg, A., Ford, R.C., 2000. The location of the mobile electron carrier ferredoxin in vascular plant photosystem I. Journal of Biological Chemistry 275, 36250–36255.

Ruffle, S.V., Mustafa, A.O., Kitmitto, A., Holzenburg, A., Ford, R.C., 2002. The location of plastocyanin in vascular plant photosystem I. Journal of Biological Chemistry 277, 25692–25696.

Ruprecht, J., Nield, J., 2001. Determining the structure of biological macromolecules by transmission electron microscopy, single particle analysis and 3D reconstruction. Progress in Biophysics and Molecular Biology 75, 121–164.

Saga, Y., Wazawa, T., Nakada, T., Ishii, Y., Yanagida, T., Tamiaki, H., 2002a. Fluorescence emission spectroscopy of single light-harvesting complex from green filamentous photosynthetic bacteria. Journal of Physical Chemistry B 106, 1430–1433.

Saga, Y., Wazawa, T., Mizoguchu, T., Ishii, Y., Yanagida, T., Tamiaki, H., 2002b. Spectral heterogeneity in single light-harvesting chlorosomes from green sulfur photosynthetic bacterium *Chlorobium tepidum*. Photochemistry and Photobiology 75, 433–436.

Saibil, H.R., 2000. Macromolecular structure determination by cryo-electron microscopy. Acta Crystallographica D 56, 1215–1222.

Sanchez, E.J., Novotny, L., Xie, X.S., 1999. Near-field fluorescence microscopy based on two-photon exciation with metal tips. Physical Review Letters 4014, 4017.

Santini, C., Tidu, V., Tognon, G., Magaldi, A.G., Bassi, R., 1994. Three-dimensional structure of the higher plant photosystem II reaction center and evidence for its dimeric organization in vivo. European Journal of Biochemistry 221, 307–315.

Sarafis, V., 1998. Cloroplasts: a structural approach. Journal of Plant Physiology 152, 248–264.

Scheuring, S., Reiss-Husson, F., Engel, A., 2001. High-resolution AFM topographs of *Rubrivivax gelatinosus* light-harvesting complex LH2. EMBO Journal 20 (12), 3029–3035.

Scheuring, S., Seguin, J., Marco, S., Levy, D., Robert, B., Rigaud, J.L., 2003a. Nanodissection and high-resolution imaging of the *Rhodopseudomonas viridis* photosynthetic core complex in native membranes by AFM. Proceedings of the National Academy of Sciences of the United States of America 100, 1690–1693.

Scheuring, S., Seguin, J., Marco, S., Levy, D., Breyton, C., Robert, B., Rigaud, J.-L., 2003b. AFM characterization of tilt and intrinsic flexibility of *Rhodobacter sphaeroides* light harvesting complex 2 (LH2). Journal of Molecular Biology 325 (3), 569–580.

Scheuring, S., Sturgis, J.N., Prima, V., Bernadac, A., Levy, D., Rigaud, J.-L., 2004a. Watching the photosynthetic apparatus in native membranes. Proceedings of the National Academy of Sciences of the United States of America 101 (31), 11293–11297.

Scheuring, S., Francia, F., Busselez, J., Melandri, B.A., Rigaud, J.L., Levy, D., 2004b. Structural role of PufX in the dimerization of the photosynthetic core complex of *Rhodobacter sphaeroides*. Journal of Biological Chemistry 279, 3620–3626.

Schmidt, Th., Schutz, G.J., Baumgartner, W., Gruber, H.J., Schindler, H., 1996. Imaging of single molecule diffusion. Proceeding of the National Academy of Sciences USA 93, 2926–2929.

Seibert, M., deWitt, M., Staehelin, A., 1987. Structural localization of the O_2-evolving apparatus to multimeric, tetrameric particles on the lumenal surfaces of freeze-etched photosynthetic membranes. Jornal of Cell Biology 105, 2257–2265.

Sepiol, J., Jasny, J., Keller, J., Wild, U.P., 1997. Single molecules observed by immersion mirror objective. Chemical Physics Letters 273, 444–448.

Shao, L., Tao, N.J., Leblanc, R.M., 1997. Probing the microelastic properties of nanobiological particles with tapping mode atomic force microscopy. Chemical Physics Letters 273 (1-2), 37–41.

Sick, B., Hecht, B., Novotny, L., 2000. Orientational imaging of single molecules by annular illumination. Physical Review Letters 85, 4482–4485.

Siebert, C.A., Qian, P., Fotiadis, D., Engel, A., Hunter, C.N., Bullough, P.A., 2004. Molecular architecture of photosynthetic membranes in *Rhodobacter sphaeroides*: the role of PufX. EMBO Journal 23, 690–700.

Staehelin, L.A., 1976. Reversible particle movements associated with unstacking and restacking of chloroplast membranes in vitro. Journal of Cell Biology 71, 136–158.

Stamouli, A., Kafi, S., Klein, D.C.G., Oosterkamp, T.H., Frenken, J.W.M., Cogdell, R.J., Aartsma, T.J., 2003. The ring structure and organization of light harvesting 2 complexes in a reconstituted lipid bilayer, resolved by atomic force microscopy. Biophysical Journal 84 (4), 2483–2491.

Stamouli, A., Frenken, J.W.M., Oosterkamp, T.H., Cogdell, R.J., Aartsma, T.J., 2004. The electron conduction of photosynthetic protein complexes embedded in a membrane. FEBS Letters 560 (1/3), 109–114.

Stoylova, S.S., Flint, T.D., Ford, R.C., Holzenburg, A., 1997. Projection structure of photosystem II in vivo determined by cryo-electron crystallography. Micron 28, 439–446.

Stoylova, S.S., Flint, T.D., Ford, R.C., Holzenburg, A., 2000. Structural analysis of photosystem II in far-red-light-adapted thylakoid membranes—new crystal forms provide evidence for a dynamic reorganization of light-harvesting antennae subunits. European Journal of Biochemistry 267, 207–215.

Subramaniam, S., Milne, J.L.S., 2004. Three-dimensional electron microscopy at molecular resolution. Annual Review of Biophysics and Biomolecular Structure 33, 141–155.

Tietz, C., Chekhlov, O., Draebenstedt, A., Schuster, J., Wrachtrup, J., 1999. Spectroscopy on single light-harvesting complexes at low temperature. Journal of Physical Chemistry B 103, 6328–6333.

Tietz, C., Gerken, U., Jelezko, F., Wrachtrup, J., 2000. Polarization measurements on single pigment–protein complexes. Single Molecules 1, 67–72.

Tietz, C., Jelezko, F., Gerken, U., Schuler, S., Schubert, A., Rogl, H., Wrachtrup, J., 2001. Single molecule spectroscopy on the light-harvesting complex II of higher plants. Biophysical Journal 556, 562.

Trudel, E., Gallant, J., Mons, S., Mioskowski, C., Lebeau, L., Jeuris, K., Foubert, P., De Schryver, F., Salesse, C., 2001. Design of functionalized lipids and evidence for their binding to photosystem II core complex by oxygen evolution measurements, atomic force microscopy, and scanning near-field optical microscopy. Biophysical Journal 81, 563–571.

Unwin, P.N.T., Henderson, R., 1975. Molecular structure determination by electron microscopy of unstained crystalline specimens. Journal of Molecular Biology 94, 425–440.

Vacha, M., Kotani, M., 2003. Three-dimensional orientation of single molecules observed by far-field and near-field fluorescence microscopy. Journal of Chemical Physics 118, 5279–5282.

Vacha, F., Vacha, M., Bumba, L., Hashizume, K., Tani, T., 2000. Inner structure of intact chloroplasts observed by a low temperature laser scanning microscope. Photosynthetica 38, 493–496.

Van der Staay, G.W.M., Boekema, E.J., Dekker, J.P., Matthijs, H.C.P., 1993. Characterization of trimeric Photosystem I particles from the prochlorophyte Prochlorothrix hollandica by electron microscopy and image analysis. Biochimica et Biophysica Acta 1142, 189–193.

Van Heel, M., Gowen, B., Matadeen, R., Orlova, E.V., Finn, R., Pape, T., Cohen, D., Stark, H., Schmidt, R., Schatz, M., Patwardhan, A., 2000. Single-particle electron cryo-microscopy, towards atomic resolution. Quarterly Review of Biophysics 33, 307–369.

Van Oijen, A.M., Koehler, J., Schmidt, J., Mueller, M., Brakenhoff, G.J., 1998a. 3-Dimensional super-resolution by spectrally selective imaging. Chemical Physics Letters 292, 183–187.

Van Oijen, A.M., Ketelaars, M., Koehler, J., Aartsma, T.J., Schmidt, J., 1998b. Spectroscopy of single light-harvesting complexes from purple photosynthetic bacteria at 1.2 K. Journal of Physical Chemistry B 102, 9363–9366.

Van Oijen, A.M., Koehler, J., Schmidt, J., Mueller, M., Brakenhoff, G.J., 1999a. Far-field fluorescence microscopy beyond the diffraction limit. Journal of the Optical Society of America A 16, 909–915.

Van Oijen, A.M., Ketelaars, M., Koehler, J., Aartsma, T.J., Schmidt, J., 1999b. Unraveling the electronic structure of individual photosynthetic pigment–protein complexes. Science 285, 400–402.

Van Oijen, A.M., Ketelaars, M., Koehler, J., Aartsma, T.J., Schmidt, J., 2000. Spectroscopy of individual light-harvesting 2 complexes of *Rhodopseudomonas acidophila*: diagonal disorder, intercomplex heterogeneity, spectral diffusion and energy transfer in the B800 band. Biophysical Journal 78 (2000), 1570–1577.

Van Spronsen, E.A., Sarafis, V., Brakenhoff, G.J., van der Voort, H.T.M., Nanninga, N., 1989. 3-Dimensional structure of living chloroplasts as visualized by confocal scanning laser microscopy. Protoplasma 148 (8–14), 1989.

Walz, T., Grigorieff, N., 1998. Electron crystallography of two-dimensional crystals of membrane proteins. Journal of Structural Biology 121, 142–161.

Wu, M., Goodwin, P.M., Ambrose, W.P., Keller, R., 1996. Photochemistry and fluorescence emission dynamics of single molecules in solution: B-phycoerythrin. Journal of Physical Chemistry 100, 17406–17409.

Yakushevska, A.E., Jensen, P.E., Keegstra, W., van Roon, H., Scheller, H.V., Boekema, E.J., Dekker, J.P., 2001. Supermolecular organization of photosystem II and its associated light-harvesting antenna in *Arabidopsis thaliana*. European Journal of Biochemistry 268, 6020–6028.

Yakushevska, A.E., Keegstra, W., Boekema, E.J., Dekker, J.P., Andersson, J., Jansson, S., Ruban, A.V., Horton, P., 2003. The structure of photosystem II in Arabidopsis. Localization of the CP26 and CP29 antenna complexes. Biochemistry 42, 608–613.

Yildiz, A., Forkey, J.N., McKinney, S.A., Ha, T., Goldman, Y.E., Selvin, P.R., 2003. Myosin V walks hand-over-hand: single fluorophore imaging with 1.5-nm localization. Science 300, 261–265.

Yildiz, A., Tomishige, M., Vale, R.D., Selvin, P.R., 2004. Kinesin walks hand-over-hand. Science 303, 676–678.

Ying, L., Xie, S., 1998. Fluorescence spectroscopy, exciton dynamics and photochemistry of single allophycocyanin trimers. Journal of Physical Chemistry B 102, 10399–10409.

Zehetmayer, P., Hellerer, Th., Parbel, A., Scheer, H., Zumbusch, A., 2002. Spectroscopy of single phycoerythrocyanin monomers: dark state identification and observation of energy transfer heterogeneities. Biophysical Journal 83, 407–415.

Zehetmayer, P., Kupka, M., Scheer, H., Zumbusch, A., 2004. Energy transfer in monomeric phycoerythrocyanin. Biochimica et Biophysica Acta 1608, 35–44.

Zhu, Y.W., Ramakrishna, B.L., van Noort, P.I., Blankenship, R.E., 1995. Microscopic and spectroscopic studies of untreated and hexanol-treated chlorosomes from *Chloroflexus aurantiacus*. Biochimica et Biophysica Acta-Bioenergetics 1232 (3), 197–207.

Zlatanova, J., Lindsay, S.M., Leuba, S.H., 2000. Single molecule force spectroscopy in biology using the atomic force microscope. Progress in Biophysics and Molecular Biology 74 (1/2), 37–61.

Zouni, A., Witt, H.T., Kern, J., Fromme, P., Krauss, N., Saenger, W., Orth, P., 2001. Crystal structure of Photosystem II from *Synechococcus elongatus* at 3.8 Å resolution. Nature 409, 739–743.